

**Fig. 7.** Activity of the mTOR/S6K Signaling Pathway Is Regulated by PKC $\zeta$  in AR-Negative Prostate Cancer Cell Lines and this Signaling Pathway Is Required for their Cell Proliferation

A, After 24 h plating in RPMI + 10% FBS, PC3, and DU145 cells were treated with 10, 20, or 50  $\mu$ M myristoylated PKC $\zeta$  pseudosubstrate inhibitor (PKC $\zeta$ PS) for 150 min. Total cell extracts were analyzed for S6K phospho-T389 (p-S6KT389), S6 phospho-S235/236 (p-S6), S6K, S6, and cyclin D1 (CCND1). The number under each lane of  $\beta$ -actin expression indicates the relative intensity of each phospho-PKC $\zeta$  expression and phospho-S6KT389 normalized to  $\beta$ -actin expression. B, Apoptosis was detected morphologically by using Hoechst 33342. PC3 cells and DU145 cells treated with 50  $\mu$ M myristoylated PKC $\zeta$  pseudosubstrate inhibitor for 12 h were collected. The cells were treated with 10% formalin neutral buffer solution, followed by rinsing with phosphate-buffer saline, and Hoechst 33342 was added at a final concentration of 0.167  $\mu$ g/ $\mu$ l and incubated for 20 min at room temperature in the dark. Cell aliquots were placed on slides and a fluorescent microscope was used to count 200 fluorescent cells per condition. Nuclear fragmentation and chromatin condensation were scored as dead. Graph represents three independent experiments in which 200 fluorescent cells were counted and scored for chromatin condensation and nuclear fragmentation.

Hence, ligand-dependent androgen hypersensitivity is not responsible for androgen-independent cell proliferation of ALLNcAP cells.

It is well known that PI3K/Akt signaling pathway participates in androgen-independent growth of prostate cancer cells (38, 51, 52). About 60% of prostate cancer patients who develop metastases have tumors in which PI3K/Akt is activated as a result of PTEN gene

mutation (53). LNCaP cells contain a frame-shift mutation in the PTEN gene and the PI3K/Akt signaling pathway is constitutively activated (53). Inhibiting PI3K/Akt signaling pathway by pharmacological agents induced apoptosis in LNCaP cells as described previously, suggesting that this signaling pathway is required for cell survival and growth in LNCaP cells (38, 52). In fact, several groups have generated andro-

**Table 1.** Relationship between Phospho-PKC $\zeta$  and Phospho-S6K Stainings of Each Cancer Spot in Tissue Microarray Derived from Clinically Localized Hormone-Naive (n = 67) (A) or Hormone-Treated (n = 12) (B) Prostate Cancer Patients<sup>a</sup>

p-PKC $\zeta$ Staining <sup>a</sup>	p-S6K Staining <sup>b</sup> : No. of Cancer Spots (%)			
	Total	-	+	++
<b>A. Hormone-Naive Patients</b>				
Total	184 (100)	42 (23)	94 (51)	48 (26)
-	19 (10)	15 (8)	4 (2)	0
+	95 (52)	27 (15)	61 (33)	7 (4)
++	70 (38)	0	29 (16)	41 (22)
<b>B. Hormone-Treated Patients</b>				
Total	29 (100)	4 (14)	15 (52)	10 (34)
-	0	0	0	0
+	13 (45)	4 (14)	7 (24)	2 (7)
++	16 (55)	0	8 (28)	8 (28)

<sup>a</sup> P < 0.01 by rank test for trend of increasing phospho-PKC $\zeta$  expression with increasing phospho-S6K expression.

<sup>b</sup> Staining of phospho-PKC $\zeta$  and phospho-S6K was classified as follows: -, no staining; +, weak; or ++, moderate to strong.

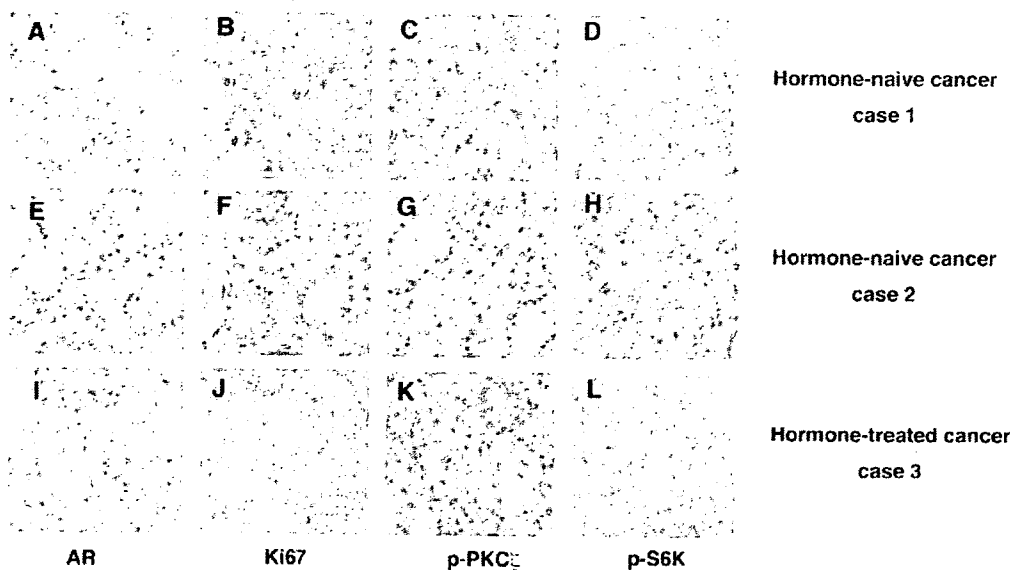


**Fig. 8.** Expression of Phospho-PKC $\zeta$  and Phospho-S6K Strongly Associates in Human Prostate Cancer Specimens

*Upper panels.* Representative immunohistochemical staining of human prostate cancer specimens from three individual patients with hormone-naïve (Cases 1 and 2) or hormone-treated prostate cancer (Case 3) for AR (A, E, and I), Ki67 (B, F, and J), phospho-PKC $\zeta$  (C, G, and K), and phospho-S6K (D, H, and L) by each specific antibody. Sections were counterstained with hematoxylin. (Case 1; A–D) Spots with Gleason 3 cancer showing moderate-to-strong (++) staining of phospho-PKC $\zeta$  and phospho-S6K. (Case 2; E–H) Spots with Gleason 3 cancer showing negative (–) staining of phospho-PKC $\zeta$  and weak (+) of phospho-S6K. (Case 3; I–L) Spots with hormonal therapy showing moderate-to-strong (++) staining of phospho-PKC $\zeta$  and phospho-S6K. Original magnification,  $\times 200$ .

gen-independent LNCaP cells through the culture of those cells in the androgen-ablated condition (17–20, 54). Pfeil *et al.* (52) reported that androgen-independent LNCaP cells were more resistant to PI3K inhibitors than parental LNCaP cells and showed higher phospho-Akt in the presence of LY294002. However, in our model, no significant activation of phospho-Akt was observed in AILNCaP cells. The expression of phospho-Akt was decreased to almost comparable level of LNCaP cells in the presence of LY294002. Shi *et al.* (20) also established three different androgen-independent LNCaP cells (LNCaP-cds). Similar to our cells, all three LNCaP-cds expressed higher level of AR without a new alternation and the amount of PSA induced by R1881 stimulation was significantly less than that of parental LNCaP cells. Although the authors did not examine the significance of signaling pathway activation in their progression to androgen-independent cell proliferation, all of LNCaP-cds expressed higher level of phospho-Akt in contrast to AILNCaP cells (20). So, mechanisms accounted for androgen-independent cell proliferation of AILNCaP cells might be different from the ones previously reported and characterized. Because Unni *et al.* (39) have reported that constitutive activation of Erk1/2 signaling through Src activation might play some role for transition of LNCaP cells to androgen independence, we first examined the phosphorylated form of Erk1/2 and p38 MAPK during acute androgen deprivation in LNCaP cells and compared their expression with AILNCaP cells under the same condition. Al-

though there was no significant difference in the phosphorylated p38 MAPK between these cell lines, expression of phosphorylated Erk1/2 was significantly elevated in AILNCaP cells. However, inhibition of Erk activity with PD98059 had no significant effect on the cell proliferation in AILNCaP cells. In addition, we showed that treatment with a myristoylated PKC $\zeta$  pseudosubstrate peptide up-regulated expression of phosphorylated Erk, whereas it impeded cell proliferation in AILNCaP cells (see the supplemental figure published as supplemental data on The Endocrine Society's Journals Online web site at <http://mend.endojournals.org>). Hence, activation of Erk1/2 observed in AILNCaP cells and in LNCaP cells under androgen deprivation may be due to a compensatory mechanism to alleviate adverse effects of various cell stresses (55). Moreover, Ravi *et al.* (56) reported that activation of ras/raf/MAPK pathway in LNCaP cells with an inducible c-raf-1 expression plasmid caused growth suppression in these cells. So, the activation of the MAPK signaling pathway does not always induce cell proliferation in LNCaP cells.

In the present report, we found for the first time that activation of the mTOR/S6 kinase pathway was regulated by androgen in LNCaP cells, whereas this pathway was activated constitutively in AILNCaP cells under androgen-depleted conditions. Treatment with rapamycin partly reduced progression from G1 to S phase in LNCaP cells cultured with normal serum and in androgen-independent AILNCaP cells under androgen deprivation. Moreover, androgen stimulation after

androgen deprivation activated the mTOR/S6 kinase pathway in the androgen-dependent LNCaP cells. These observations suggest that mTOR/S6 kinase pathway was activated by stimulation of androgen in LNCaP cells and constitutive activation of pathway was related to androgen-independent cell proliferation in AILNCaP cells. Recent studies by Ghosh *et al.* (57) reported that mTOR-S6 kinase activation is important for cell proliferation in androgen-independent prostate cancer cells. They also showed that activity of S6 kinase was higher in C4-2 cells in comparison to LNCaP cells in response to growth factor stimulation. Under normal cell growth condition, our results demonstrated that there was no significant difference in the S6 kinase activity between LNCaP and AILNCaP cells. Furthermore, they showed that rapamycin inhibited cell proliferation of C4-2 cells but not of LNCaP cells, which was different from our results. This might be due to difference in some experimental conditions. For instance, our treatment with rapamycin was extended for 72 h before harvesting the cells for analysis in cell cycle distribution, whereas their treatment with rapamycin was for 48 h.

To clarify the roles of androgen stimulation in activating mTOR/S6K pathway, we investigate the activities of various known upstream signaling pathways and demonstrate that activation of PKC $\zeta$  is responsible for mTOR/S6K activation in both cells. Androgen deprivation reduced the activity of PKC $\zeta$  in LNCaP cells, whereas androgen stimulation partially restored this activity. On the other hand, PKC $\zeta$  was activated in AILNCaP cells and these cells showed twice as much PKC $\zeta$  kinase activity than that of LNCaP cells in androgen-deprived condition. To demonstrate the requirement for higher PKC $\zeta$  kinase activity for androgen-independent cell proliferation and S6K activation in AILNCaP, we examined the effect of a specific inhibitor of PKC $\zeta$ , a myristoylated PKC $\zeta$  pseudosubstrate peptide on these cells. Treatment with 20  $\mu$ M myristoylated PKC $\zeta$  pseudosubstrate peptide induced 20% decrease in PKC $\zeta$  kinase activity (data not shown) and this decrease resulted in 50% reduction of cell population in S phase, 40% reduction of phospho-S6K expression, and inducing apoptosis in AILNCaP cells. These results also suggested that twice as much difference of endogenous PKC $\zeta$  kinase activity between AILNCaP and LNCaP cells in androgen-deprived condition was significant. This result is consistent with our recent results in that 2-fold difference of endogenous PKC $\zeta$  kinase activity was sufficient to influence the conformation of AP-1 family protein such as JunB in renal cell carcinoma cell lines (58). Inhibition of PKC $\zeta$  kinase activity also reduced phospho-S6K expression (Fig. 7A) and cell proliferation (data not shown), and induced apoptosis in AR-negative prostate cancer cell lines, PC3 and DU145. So, this activity is also required for cell proliferation of these cells. As for the reasons why mere androgen stimulation partially restored S6K and PKC $\zeta$  activity in LNCaP cells, we speculate that the possibility that other steroids

ablated in CSFBS may also participate in the activation of these kinases. The precise mechanism for this is currently under our investigation.

As for functional relationship between PKC $\zeta$  and S6K, the association of transfected PKC $\zeta$  and S6K was observed in LNCaP, and this association was enhanced by androgen stimulation in LNCaP cell. We also revealed that the inhibition of endogenous PKC $\zeta$  activity did induce the reduction of endogenous phosphorylation of S6K. Although the association of endogenous protein was not confirmed, these results indicate the possibility that PKC $\zeta$  can associate with S6K in LNCaP cells in similar ways that was previously reported in HEK 293 cells (29) and androgen stimulation enhanced this association in LNCaP cells. Because the amount of S6K protein decreased under androgen depleted conditions, there is also a possibility that expression of S6K is regulated by PKC $\zeta$  in mRNA or protein level (59). The precise roles in LNCaP cells remained to be clarified.

In LNCaP cells, 0.1 nM of R1881 stimulation activated PKC $\zeta$ /S6K signaling pathway, whereas mere supplementation of R1881 with charcoal-stripped serum only modestly induced cell proliferation. Although 10 nM of R1881 stimulation activated PKC $\zeta$ /S6K, it did not induce cell proliferation effectively in LNCaP cells. This discrepancy suggests that other signaling pathways also control cell proliferation of LNCaP cells (60, 61).

Treatment with the specific AR inhibitor, bicalutamide, together with R1881 attenuated PKC $\zeta$  and S6K phosphorylation in LNCaP cells, indicating that the androgen/androgen-receptor complex participated in this signaling activation. Our data suggested a few possible mechanisms of androgen action to activate PKC $\zeta$ : 1) androgen stimulation regulates PKC $\zeta$  phosphorylation, probably through another PKC $\zeta$  kinase; 2) androgen stimulation stabilizes PKC $\zeta$  by regulating scaffold proteins such as molecular chaperones, or by inhibiting degradation pathways; and 3) androgen stimulation regulates a phosphatase that inactivates PKC $\zeta$ . The precise mechanisms remained to be clarified.

Interestingly, recent evidence suggests that PKC $\zeta$  is involved in estradiol-activated signaling pathways regulated by a classic steroid receptor without exerting a transcriptional effect in a human breast cancer cell line, MCF-7 (62). Thus, based on this previous report, important issues are raised whether androgen/AR complex participates in this signaling activation through genomic or nongenomic action (63, 64). Castoria *et al.* (62) revealed that stimulation with estradiol for 3 min activates PKC $\zeta$  in MCF-7 cells and described that this nongenomic action of steroid receptors facilitates the Src-dependent Ras activation through PKC $\zeta$ . The Src-dependent Ras activation also occurred by 2- to 5-min androgen stimulation in LNCaP cells (39, 65). In our model, R1881 treatment did not induce any apparent increase either in PKC $\zeta$  (T410) or S6K (T389) phosphorylation within 6 h, whereas it

significantly induced an increase in phosphorylation of both PKC $\zeta$  and S6K after 24 h (data not shown). The induction of PSA was observed after 6 h at 10 nM of R1881 (data not shown). These results implied that slow receptor transcriptional activity rather than rapid signaling activation participates in PKC $\zeta$  activation in LNCaP cells. However, these results do not exclude the possibilities of nongenomic action of AR definitively and they remain to be clarified.

In conclusion, we demonstrate for the first time that the androgen/androgen-receptor complex activates the mTOR/S6K pathways through PKC $\zeta$  in LNCaP cells and constitutive activation of this pathway is related to transition of LNCaP cells to androgen-independent cell proliferation. We also show that both S6K and PKC $\zeta$  are activated in considerable numbers of hormone-naïve prostate cancer cells *in vivo*, and their activation is correlated with each other. Furthermore, activation of both kinases positively correlated with the expression of Ki67, which is a good indicator of cell proliferation (49), supporting the *in vitro* results. As for hormone-treated prostate cancer specimens, we analyzed residual viable cancer cells in the specimen. So, most of them might be a transition state in the continuum between hormone-naïve prostate cancer and full-blown hormone-refractory cancer cells (50). Interestingly, 86% of spots were positively stained with both phospho-PKC $\zeta$  and phospho-S6K antibodies. We did not exclude the possibilities that some of these cells acquired hypersensitivity to androgen, and the number of hormone-treated prostate cancer specimen is too small to evaluate the significance of activation of PKC $\zeta$ /S6K pathway definitively. However, these results implied the possibility that activation PKC $\zeta$ -mTOR/p70 S6 kinase pathway may be associated with transition of hormone-naïve prostate cancer cells to androgen-independent growth or survival also *in vivo*.

## MATERIALS AND METHODS

### Antibodies and Reagents

Anti-phospho-Akt (S473), anti-phospho-p70S6K (T389), anti-phospho-p70S6K (S371), anti-phospho-S6 (S235/236), anti-phospho-p44/42 MAPK (T202/Y204), anti-phospho-p38 MAPK (T180/Y182), anti-phospho-PDK1 (S241), anti-phospho-TSC2 (T1426), anti-Akt, anti-S6, anti-p44/42 MAPK, and anti-p38 MAPK antibodies were obtained from Cell Signaling Technology (Beverly, MA). Anti-PDK1, anti-AR, anti-PSA, anti-TSC2, anti-phospho-PKC $\zeta$  (T410), anti-c-myc, anti-PKC $\zeta$  and anti-S6K were obtained from Santa Cruz Biotechnology (Santa Cruz, CA). Anti-cyclin D1 was obtained from Novocastra (Newcastle, UK). Anti- $\beta$ -actin was purchased from Abcam (Cambridge, UK), and anti-HA, from Covance (Berkeley, CA). LY294002, rapamycin, PD98059 and myristoylated PKC $\zeta$  pseudosubstrate inhibitor were purchased from Calbiochem (San Diego, CA). Wortmannin and hydroxyflutamide were obtained from Sigma (St. Louis, MO), and bicalutamide, from Toronto Research Chemicals (Toronto, Ontario, Canada). Hoechst 33342 was obtained from Wako (Kumamoto,

Japan). R1881 (methyltrienolone) was purchased from Dupont Merck Pharmaceutical (Boston, MA).

### Cell Culture

The prostate cancer cell lines LNCaP, PC3, DU145, and HEK 293 were obtained from the American Type Culture Collection (Rockville, MD). The cells were cultured routinely in RPMI (Invitrogen, Carlsbad, CA) or DMEM (Invitrogen) supplemented with 10% FBS at 37 C in incubators with humidified air and 5% carbon dioxide. The subline AILNCaP was established by maintaining LNCaP cells in phenol red-free RPMI (Invitrogen) supplemented with 10% CSFBS (Hyclone, Logan, UT), with a change of this steroid-free medium every 3–4 d over 3 months as described previously (38, 59). Although more than 99% of cells underwent apoptosis during 3 months of cell culture in CSFBS, the remaining new cell line, AILNCaP, begun to grow after this 3-month period and was maintained in phenol red-free RPMI (Invitrogen) supplemented with 10% CSFBS being passaged at 70% confluence by trypsinization, for another 6 months.

### Flow Cytometry

Control and treated cells were harvested by 1 ml of 0.05% trypsin-EDTA for 3 min at 37 C to detach them from the plastic surface. Cells were centrifuged, washed in PBS, and then fixed by slow addition of 3 ml of ice-cold 70% ethanol with mild shaking; they then were stored at 4 C until use. On the day of cycle analysis, the cells were centrifuged, washed in PBS, resuspended in 1 ml per  $10^6$  cells of PBS containing 100  $\mu$ g/ml RNase A (QIAGEN, Hilden, Germany) and 0.25  $\mu$ g/ml of 7-amino-actinomycin D (BD Biosciences, San Diego, CA), and incubated at 37 C for 30 min. To determine DNA content, at least 10,000 cells were analyzed with a FACSCalibur flow cytometer using CellQuest software (BD Biosciences).

### Quantitative RT-PCR

Total cellular RNA was isolated with RNeasy Mini Kit (QIAGEN), and cDNA was synthesized from 2  $\mu$ g of total RNAs with random primers using First-Strand cDNA Synthesis Kit (Amersham Pharmacia Biotech, Piscataway, NJ) according to the manufacturer's instruction. PCR was performed by SYBR green PCR Master Mix (Applied Biosystems, Foster City, CA) as described using the relative standard curve method (66). The increase in fluorescence of the SYBR green dye was monitored using GeneAmp 5700 sequence detection system (Applied Biosystems). All of the PCRs were performed in triplicate. The values were normalized to the amounts of TATA-binding protein. The sequences of primers used for PCR analyses are as follows: PSA, 5'-GGAAATGAC-CAGGCCAAGAC-3' (sense) and 5'-CAACCCTGGACCTCACACCTA-3' (antisense), TATA-binding protein (TATABP), 5'-GAATATAATCCCAAGCGGTTTG-3' (sense) and 5'-ACTTCCACATCACAGCTCCCC-3' (antisense). Conventional PCR was conducted with the following profile: initial heating to 95 C for 10 min followed by 37 PCR cycles of denaturing at 95 C for 45 sec, annealing at 60 C for 45 sec, and extension at 72 C for 45 sec for both PSA and TATABP. The amplified products were visualized on 1.8% agarose gels.

### Cell Lysis and Immunoblotting

After washing with ice-cold PBS, cells were harvested in lysis buffer containing 50 mM Tris-HCl (pH 7.4), 1% Triton X-100, 150 mM sodium chloride, 2 mM EDTA, 1 mM EGTA, 0.2 mM sodium vanadate, 50 mM sodium fluoride, 1 mM dithiothreitol, and 1 mM phenylmethylsulfonyl fluoride supplemented with

protease cocktail inhibitors (Complete Mini; Roche, Mannheim, Germany). Whole-cell extracts were centrifuged at  $13,000 \times g$  at 4 C for 20 min. Total cellular protein concentrations were determined by using a protein assay reagent (Bio-Rad, Richmond, CA). Lysates were subjected to SDS-PAGE, transferred to polyvinylidene difluoride membranes (Millipore, Bedford, MA). Membranes were immunoblotted with primary antibodies followed by horseradish peroxidase-conjugated secondary antibodies, and developed for reading by enhanced chemiluminescence (Amersham Pharmacia Biotech). Densitometric analysis was performed by Image J software (National Institutes of Health, Bethesda, MD). All blots were stained with Ponceau S to confirm equal protein loading.

### Transfection and Immunoprecipitation

Transfection was performed in DMEM or RPMI with or without 10% FBS using Lipofectamine 2000 reagent (Invitrogen) according to the manufacturer's instructions. Cells were lysed in lysis buffer [50 mM Tris-HCl (pH 7.4), 150 mM NaCl, 0.5% (vol/vol) Nonidet P-40, 5 mM EDTA] containing 2 mM orthovanadate, 5 mM NaF, 1 mM phenylmethylsulfonyl fluoride, and protease cocktail inhibitor, and immunoprecipitated with the antibody indicated and protein G-Sepharose beads (Amersham, Buckinghamshire, UK). Immune complexes were subjected to SDS-PAGE and Western blotting.

### Expression Constructs

PKC $\zeta$ -myc was generated by subcloning wild-type human PKC $\zeta$  into the *KpnI* and *EcoRI* sites of the mammalian expression vector pcDNA3.1/*myc*-His A (Invitrogen). All constructs were amplified by PCR, and DNA sequences were verified using ABI PRISM 310 genetic analyzer. HA-p70S6K wild-type was kindly provided by Dr. John Blenis (Department of Cell Biology, Harvard Medical School, Boston, MA).

### Immunocomplex Kinase Assay

Cells in the growth phase were washed with PBS and lysed in lysis buffer [50 mM Tris-HCl (pH 7.4), 150 mM NaCl, 0.5% (vol/vol) Nonidet P-40, 5 mM EDTA] containing 2 mM orthovanadate, 5 mM NaF, 1 mM phenylmethylsulfonyl fluoride, and protease cocktail inhibitor. Activity of S6 kinase was determined using a S6 kinase assay kit (Upstate Biotechnology, Lake Placid, NY) according to the manufacturer's instructions with some modification. Briefly, 10  $\mu$ l of assay dilution buffer [ADB: 20 mM 3[(*N*-morpholino)propanesulfonic acid (pH 7.2), 25 mM  $\beta$ -glycerol phosphate, 5 mM EGTA, 1 mM sodium orthovanadate, and 1 mM dithiothreitol], 10  $\mu$ l of substrate cocktail [250  $\mu$ M substrate peptide (AKRRRLSSLRA) in ADB], 10  $\mu$ l of inhibitor cocktail, 10  $\mu$ l of the [ $\gamma$ - $^{32}$ P] ATP mixture (magnesium/ATP cocktail including 10  $\mu$ Ci of [ $\gamma$ - $^{32}$ P] ATP) and immunoprecipitate with S6 kinase polyclonal antibody (Santa Cruz) were mixed and incubated for 10 min at 37 C. For assay of PKC $\zeta$  activity, lysates were prepared similarly, immunoprecipitated with PKC $\zeta$  polyclonal antibody, and then incubated for 20 min at 30 C in 50  $\mu$ l of kinase assay mixture as described previously (35). In all kinase reactions,  $^{32}$ P incorporation into substrates was measured by liquid scintillation counting.

### Prostate Cancer Tissue Microarray and Immunohistochemistry

Prostate cancer tissues evaluated were derived from radical prostatectomy specimens of 79 localized prostate cancer patients at Kyoto University Hospital. Using these specimen TMAs were constructed as previously described (49). Stan-

dard indirect immunoperoxidase procedures using monoclonal and polyclonal antibodies were applied to detect AR (1:100, 2F12 Novocastra), Ki67 (1:100, MIB-1, DAKO, Kyoto, Japan), phospho-p70S6K (T389) (1:50; Cell Signaling Technology), and phospho-PKC $\zeta$  (T410) (1:100; Santa Cruz). Adjacent sections within 15  $\mu$ M of TMAs were used for the analysis. Available cancer spots were 213 spots. Immunopositivity of phospho-p70S6K and phospho-PKC $\zeta$  was graded as (-) (no staining), (+) (weak immunostaining involving less than 50%), (+ +) (moderate-to-strong immunostaining involving more than 50%) by two of the authors (T. I. and Y.S.), independently. The Ki67 labeling index was determined as described previously (49). All the patients involved in this study provided informed consent.

### Statistical analyses

Data are presented as mean  $\pm$  SD. Means were considered as statistically different, *i.e.*  $P < 0.05$ , which was determined by one-way ANOVA and the least significant multiple comparison method. Spearman's rank order correlation analysis was used to analyze the statistical significance of the correlations among phospho-S6K and phospho-PKC $\zeta$  expression in cancer spots.

### Acknowledgments

We thank Dr. John Blenis (Department of Cell Biology, Harvard Medical School, Boston, MA) for supplying pRK7 HAS6K-1. We also thank all members of Cancer Research Course in Graduated Courses for Integrated Research Training, Kyoto University Faculty of Medicine, the Ogawa's lab, and Dr. Tomomi Yamada (Division of Medical Informatics, Kyusyu University Hospital) for helpful discussion. We thank the skillful technical assistance of Tomoko Matsushita and Chie Hagihara (Department of Urology, Kyoto University).

Received January 19, 2006. Accepted August 14, 2006.

Address all correspondence and requests for reprints to: Eijiro Nakamura, M.D., Ph.D., Department of Urology, Kyoto University Graduate School of Medicine, 54 Kawaharacho, Shogoin, Sakyo-ku, Kyoto 606-8507, Japan. E-mail: hap@kuhp.kyoto-u.ac.jp.

This work was supported by a Grant-in-Aid from Ministry of Education, Culture, Sports, Science and Technology, Japan, Yamaguchi Endocrine Research Association, the Japanese Foundation for Prostate Research, Organon Urology Academia, and Formation for Genomic Analysis of Disease Model Animals with Multiple Genetic (Center of Excellence program), Ministry of Education, Culture, Sports, Science and Technology, Japan.

Disclosure Statement: The authors have nothing to disclose.

### REFERENCES

- Huggins C, Hodges CV 1941 Studies on prostatic cancer: effect of castration, of estrogen and of androgen injection on serum phosphatases in metastatic carcinoma of the prostate. *Cancer Res* 1:293–297
- Gelmann EP 2002 Molecular biology of the androgen receptor. *J Clin Oncol* 20:3001–3015
- Chen CD, Welsbie DS, Tran C, Baek SH, Chen R, Vessella R, Rosenfeld MG, Sawyers CL 2004 Molecular determinants of resistance to antiandrogen therapy. *Nat Med* 10:33–39

4. Feldman BJ, Feldman D 2001 The development of androgen-independent prostate cancer. *Nat Rev Cancer* 1:34–45
5. Visakorpi T, Hyytinen E, Koivisto P, Tanner M, Keinänen R, Palmberg C, Palotie A, Tammela T, Isola J, Kallioniemi OP 1995 In vivo amplification of the androgen receptor gene and progression of human prostate cancer. *Nat Genet* 9:401–406
6. Gregory CW, Johnson RT, Mohler JL, French FS, Wilson, EM 2001 Androgen receptor stabilization in recurrent prostate cancer is associated with hypersensitivity to low androgen. *Cancer Res* 61:2892–2892
7. Taplin ME, Bublely GJ, Shuster TD, Frantz ME, Spooner AE, Ogata GK, Keer HN, Balk SP 1995 Mutation of the androgen-receptor gene in metastatic androgen-independent prostate cancer. *N Engl J Med* 332:1393–1398
8. Han G, Buchanan G, Iltmann M, Harris JM, Yu X, Demayo FJ, Tilley W, Greenberg NM 2005 Mutation of the androgen receptor causes oncogenic transformation of the prostate. *Proc Natl Acad Sci USA* 102:1151–1156
9. Miyamoto H, Yeh S, Wilding G, Chang C 1998 Promotion of agonist activity of antiandrogens by the androgen receptor coactivator, ARA70, in human prostate cancer DU145 cells. *Proc Natl Acad Sci USA* 95:7379–7384
10. Culig Z, Hobisch A, Cronauer MV, Radmayr C, Trapman J, Hittmair A, Bartsch G, Klocker H 1994 Androgen receptor activation in prostatic tumor cell lines by insulin-like growth factor-I, keratinocyte growth factor, and epidermal growth factor. *Cancer Res* 54:5474–5478
11. Kiyama S, Morrison K, Zellweger T, Akbari M, Cox M, Yu D, Miyake H, Gleave ME 2003 Castration-induced increases in insulin-like growth factor-binding protein 2 promotes proliferation of androgen-independent human prostate LNCaP tumors. *Cancer Res* 63:3575–3584
12. Craft N, Shostak Y, Carey M, Sawyers CL 1999 A mechanism for hormone-independent prostate cancer through modulation of androgen receptor signaling by the HER-2/neu tyrosine kinase. *Nat Med* 5:280–285
13. McDonnell TJ, Troncoso P, Brisbay SM, Logothetis C, Chung LWK, Hsieh JT, Tu SM, Campbell ML 1992 Expression of the protooncogene bcl-2 in the prostate and its association with emergence of androgen-independent prostate cancer. *Cancer Res* 52:6940–6944
14. Gleave M, Tolcher A, Miyake, Nelson C, Brown B, Beraldi E, Goldie J 1999 Progression to androgen independence is delayed by adjuvant treatment with antisense Bcl-2 oligodeoxynucleotides after castration in the LNCaP prostate tumor model. *Clin Cancer Res* 5:2891–2898
15. Horoszewicz JS, Leong SS, Kawinski E, Karr JP, Rosenthal H, Chu TM, Mirand EA, Murphy GP 1983 LNCaP model of human prostatic carcinoma. *Cancer Res* 43:1809–1818
16. Lee C, Sutkowski DM, Sensibar JA, Zelner D, Kim I, Arnsel I, Shaw N, Prins GS, Kozlowski JM 1995 Regulation of proliferation and production of prostate-specific antigen in androgen-sensitive prostatic cancer cells, LNCaP, by dihydrotestosterone. *Endocrinology* 136:796–803
17. Culig Z, Hoffmann J, Erdel M, Eder IE, Hobisch A, Hittmair A, Bartsch G, Utermann G, Schneider MR, Parczyk K, Klocker H 1999 Switch from antagonist to agonist of the androgen receptor bicalutamide is associated with prostate tumour progression in a new model system. *Br J Cancer* 81:242–251
18. Igawa T, Lin FF, Lee MS, Karan D, Batra SK, Lin MF 2002 Establishment and characterization of androgen-independent human prostate cancer LNCaP cell model. *Prostate* 50:222–235
19. Wang LG, Ossowski L, Ferrari AC 2001 Overexpressed androgen receptor linked to p21WAF1 silencing may be responsible for androgen independence and resistance to apoptosis of a prostate cancer cell line. *Cancer Res* 61:7544–7551
20. Shi XB, Ma AH, Tepper CG, Xia L, Gregg JP, Gandour-Edwards R, Mack PC, Kung HJ, DeVere White RW 2004 Molecular alterations associated with LNCaP cell progression to androgen independence. *Prostate* 60:257–271
21. Jacinto E, Hall MN 2003 Tor signalling in bugs, brain and brawn. *Nat Rev Mol Cell Biol* 4:117–126
22. Inoki K, Ouyang H, Li Y, Guan KL 2005 Signaling by target of rapamycin proteins in cell growth control. *Microbiol Mol Biol Rev* 69:79–100
23. Inoki K, Corradetti MN, Guan KL 2005 Dysregulation of the TSC-mTOR pathway in human disease. *Nat Genet* 37:19–24
24. Fingar DC, Richardson CJ, Tee AR, Cheatham L, Tsou C, Blenis J 2004 mTOR controls cell cycle progression through its cell growth effectors S6K1 and 4E-BP1/eukaryotic translation initiation factor 4E. *Mol Cell Biol* 24:200–216
25. Lane HA, Fernandez A, Lamb NJ, Thomas G 1993 p70s6k function is essential for G1 progression. *Nature* 363:170–172
26. Martin KA, Blenis J 2002 Coordinate regulation of translation by the PI 3-kinase and mTOR pathways. *Adv Cancer Res* 86:1–39
27. Chou MM, Blenis J 1996 The 70 kDa S6 kinase complexes with and is activated by the Rho family G proteins Cdc42 and Rac1. *Cell* 85:573–583
28. Pullen N, Dennis PB, Andjelkovic M, Dufner A, Kozma SC, Hemmings BA, Thomas G 1998 Phosphorylation and activation of p70s6k by PDK1. *Science* 279:707–710
29. Romanelli A, Martin KA, Toker A, Blenis J 1999 p70 S6 kinase is regulated by protein kinase C  $\zeta$  and participates in a phosphoinositide 3-kinase-regulated signalling complex. *Mol Cell Biol* 19:2921–2928
30. Akimoto K, Nakaya M, Yamanaka T, Tanaka J, Matsuda S, Weng Q, Avruch J, Ohno, S 1998 Atypical protein kinase Clambda binds and regulates p70 S6 kinase. *Biochem J* 335:417–424
31. Chou MM, Hou W, Johnson J, Graham LK, Lee MH, Chen CS, Newton AC, Schaffhausen BS, Toker A 1998 Regulation of protein kinase C  $\zeta$  by PI 3-kinase and PDK-1. *Curr Biol* 8:1069–1077
32. Le Good JA, Ziegler WH, Parekh DB, Alessi DR, Cohen P, Parker PJ 1998 Protein kinase C isoforms controlled by phosphoinositide 3-kinase through the protein kinase PDK1. *Science* 281:2042–2045
33. Nakanishi H, Exton JH 1992 Purification and characterization of the zeta isoform of protein kinase C from bovine kidney. *J Biol Chem* 267:16347–16354
34. Parekh DB, Ziegler W, Parker PJ 2000 Multiple pathways control protein kinase C phosphorylation. *EMBO J* 19:496–503
35. Takeda H, Matozak T, Takada T, Noguchi T, Yamao T, Tsuda M, Ochi F, Fukunaga K, Inagaki K, Kasuga M 1999 PI 3-kinase  $\gamma$  and protein kinase C- $\zeta$  mediate RAS-independent activation of MAP kinase by a Gi protein-coupled receptor. *EMBO J* 18:386–395
36. Scott MT, Ingram A, Ball KL 2002 PDK1-dependent activation of atypical PKC leads to degradation of the p21 tumour modifier protein. *EMBO J* 21:6771–6780
37. Knudsen KE, Arden KC, Cavenee WK 1998 Multiple G1 regulatory elements control the androgen-dependent proliferation of prostatic carcinoma cells. *J Biol Chem* 273:20213–20222
38. Murillo H, Huang H, Schmidt LJ, Smith DI, Tindall DJ 2001 Role of PI3K signaling in survival and progression of LNCaP prostate cancer cells to the androgen refractory state. *Endocrinology* 142:4795–4805
39. Unni E, Sun S, Nan B, McPhaul MJ, Cheskis B, Mancini MA, Marcelli M 2004 Changes in androgen receptor nongenotropic signaling correlates with transition of LNCaP cells to androgen independence. *Cancer Res* 64:7156–7168

40. Gioeli D, Mandell JW, Petroni GR, Frierson Jr HF, Weber MJ 1999 Activation of mitogen-activated protein kinase associated with prostate cancer progression. *Cancer Res* 59:279–284
41. Bakin RE, Gioeli D, Sikes RA, Bissonette EA, Weber MJ 2003 Constitutive activation of the Ras/mitogen-activated protein kinase signaling pathway promotes androgen hypersensitivity in LNCaP prostate cancer cells. *Cancer Res* 63:1981–1989
42. Weng QP, Andrabi K, Kozlowski MT, Grove JR, Avruch J 1995 Multiple independent inputs are required for activation of the p70 S6 kinase. *Mol Cell Biol* 15:2333–2340
43. Burnett PE, Barrow RK, Cohen NA, Snyder SH, Sabatini DM 1998 RAFT1 phosphorylation of the translational regulators p70 S6 kinase and 4E-BP1. *Proc Natl Acad Sci USA* 95:1432–1437
44. Chung J, Grammer TC, Lemon KP, Kazlauskas A, Blenis J 1994 PDGF- and insulin-dependent pp70S6k activation mediated by phosphatidylinositol-3-OH kinase. *Nature* 370:71–75
45. Sekulic A, Hudson CC, Homme JL, Yin P, Otterness DM, Karnitz LM, Abraham RT 2000 A direct linkage between the phosphoinositide 3-kinase-AKT signaling pathway and the mammalian target of rapamycin in mitogen-stimulated and transformed cells. *Cancer Res* 60:3504–3513
46. Dan HC, Sun M, Yang L, Feldman RI, Sui XM, Ou CC, Nellist M, Yeung RS, Halley DJ, Nicosia SV, Pledger WJ, Cheng JQ 2002 Phosphatidylinositol 3-kinase/Akt pathway regulates tuberous sclerosis tumor suppressor complex by phosphorylation of tuberlin. *J Biol Chem* 277:35364–35370
47. Inoki K, Li Y, Zhu T, Wu J, Guan KL 2002 TSC2 is phosphorylated and inhibited by Akt and suppresses mTOR signalling. *Nat Cell Biol* 4:648–657
48. Ghosh PM, Bedolla R, Mikhailova M, Kreisberg JI 2002 RhoA-dependent murine prostate cancer cell proliferation and apoptosis: role of protein kinase C $\zeta$ . *Cancer Res* 62:2630–2636
49. Inoue T, Segawa T, Shiraishi T, Yoshida T, Toda Y, Yamada T, Kinukawa N, Kinoshita H, Kamoto T, Ogawa O 2005 Androgen receptor, Ki67, and p53 expression in radical prostatectomy specimens predict treatment failure in Japanese population. *Urology* 66:332–337
50. Signoretti S, Montironi R, Manola J, Altinari A, Tam C, Bublely G, Balk S, Thomas G, Kaplan I, Hlatky L, Hahnfeldt P, Kantoff P, Loda M 2000 Her-2-neu expression and progression toward androgen independence in human prostate cancer. *J Natl Cancer Inst* 92:1918–1925
51. Gao N, Zhang Z, Jiang BH, Shi X 2003 Role of PI3K/AKT/mTOR signaling in the cell cycle progression of human prostate cancer. *Biochem Biophys Res Commun* 310:1124–1132
52. Pfeil K, Eder IE, Putz T, Ramoner R, Culig Z, Ueberall F, Bartsch G, Klocker H 2004 Long-term androgen-ablation causes increased resistance to PI3K/Akt pathway inhibition in prostate cancer cells. *Prostate* 58:259–268
53. Sansal I, Sellers WR 2004 The biology and clinical relevance of the PTEN tumor suppressor pathway. *J Clin Oncol* 22:2954–2963
54. Kokontis JM, Hsu S, Chuu C, Dang M, Fukuchi J, Hiipakka RA, Liao S 2005 Role of androgen receptor in the progression of human prostate tumor cells to androgen independence and insensitivity. *Prostate* 65:287–298
55. Fang L, Li G, Liu G, Lee SW, Aaronson SA 2001 p53 Induction of heparin-binding EGF-like growth factor counteracts p53 growth suppression through activation of MAPK and PI3K/Akt signaling cascades. *EMBO J* 20:1931–1939
56. Ravi RK, McMahon M, Yangang Z, Williams JR, Dillehay LE, Nelkin BD, Mabry M 1999 Raf-1-induced cell cycle arrest in LNCaP human prostate cancer cells. *J Cell Biochem* 72:458–469
57. Ghosh PM, Malik SN, Bedolla RG, Wang Y, Mikhailova M, Prihoda TJ, Troyer DA, Kreisberg JI 2005 Signal transduction pathways in androgen-dependent and -independent prostate cancer cell proliferation. *Endocr Relat Cancer* 12:119–134
58. Lee S, Nakamura E, Yang H, Wei W, Linggi MS, Sajan MP, Farese RV, Freeman RS, Carter BD, Kaelin Jr WG, Schlisio S 2005 Neuronal apoptosis linked to EglN3 prolyl hydroxylase and familial pheochromocytoma genes: developmental culling and cancer. *Cancer Cell* 8:155–167
59. Hernandez-Pigeon H, Quillet-Mary A, Louat T, Schambourg A, Humberto O, Selves J, Salles B, Laurent G, Lautier D 2005 hMutS  $\alpha$  is protected from ubiquitin-proteasome-dependent degradation by atypical protein kinase C  $\zeta$  phosphorylation. *J Mol Biol* 348:63–74
60. Geck P, Maffini MV, Szelei J, Sonnenschein C, Soto AM 2000 Androgen-induced proliferative quiescence in prostate cancer cells: the role of AS3 as its mediator. *Proc Natl Acad Sci USA* 97:10185–10190
61. Soto AM, Sonnenschein C 2001 The two faces of janus: sex steroids as mediators of both cell proliferation and cell death. *J Natl Cancer Inst* 93:1673–1675
62. Castoria G, Migliaccio A, Di Domenico M, Lombardi M, de Falco A, Varricchio L, Bilancio A, Barone MV, Auricchio F 2004 Role of atypical protein kinase C in estradiol-triggered G1/S progression of MCF-7 cells. *Mol Cell Biol* 24:7643–7653
63. Heinlein C, Chang C 2002 The roles of androgen receptors and androgen-binding proteins in nongenomic androgen actions. *Mol Endocrinol* 18:2181–2187
64. Freeman MR, Cinar B, Lu ML 2005 Membrane rafts as potential sites of nongenomic hormonal signaling in prostate cancer. *Trends Endocrinol Metab* 16:273–279
65. Migliaccio A, Castoria G, Di Domenico M, deFalco A, Bilancio A, Lombardi M, Barone MV, Ametrano D, Zanini MS, Abbondanza C, Auricchio F 2000 Steroid-induced androgen receptor-oestradiol receptor  $\beta$ -Src complex triggers prostate cancer cell proliferation. *EMBO J* 19:5406–5417
66. Inoue T, Nakanishi H, Inada K, Hioki T, Tatematsu M, Sugimura Y 2001 Real time reverse transcriptase polymerase chain reaction of urinary cytokeratin 20 detects transitional cell carcinoma cells. *J Urol* 166:2134–2141

**Molecular Endocrinology** is published monthly by The Endocrine Society (<http://www.endo-society.org>), the foremost professional society serving the endocrine community.

## Quantitative Detection of Micrometastases in Pelvic Lymph Nodes in Patients with Clinically Localized Prostate Cancer by Real-time Reverse Transcriptase-PCR

Hideaki Miyake,<sup>1</sup> Isao Hara,<sup>1</sup> Toshifumi Kurahashi,<sup>1</sup> Taka-aki Inoue,<sup>2</sup> Hiroshi Eto,<sup>2</sup> and Masato Fujisawa<sup>1</sup>

**Abstract** **Purpose:** Routine pathologic examination can miss micrometastatic tumor foci in the lymph nodes of patients with prostate cancer, resulting in confusion during tumor staging and clinical decision-making. The objective of this study was to clarify the significance of micrometastases in pelvic lymph nodes in patients who underwent radical prostatectomy for prostate cancer. **Experimental Design:** The expression of prostate-specific antigen (PSA) and prostate-specific membrane antigen (PSMA) in 2,215 lymph nodes isolated from 120 patients with clinically localized prostate cancer was assessed by a fully quantitative real-time reverse transcriptase-PCR. We regarded specimens in which either PSA or PSMA mRNAs were positive as proof of the "presence of micrometastasis." Immunohistochemical staining of lymph node specimens with an antibody against PSA was also done. **Results:** Pathologic examinations detected tumor cells in 29 lymph nodes from 11 patients, and real-time reverse transcriptase-PCR further identified micrometastasis in 143 lymph nodes from 32 patients with no pathologic evidence of lymph node involvement. The presence of micrometastatic cancer cells was confirmed by immunohistochemical staining in 61 lymph nodes from 17 patients with pathologically negative lymph nodes. The presence of micrometastases was significantly associated with other conventional prognostic variables, including serum PSA value, pathologic stage, Gleason score, and tumor volume. Biochemical recurrence was detected in 32 patients, 17 of whom were negative for lymph node metastasis by pathologic examination (including 4 patients with pathologically organ-confined disease), but were diagnosed as having micrometastasis. Biochemical recurrence-free survival rate in patients without micrometastasis was significantly higher than in those with micrometastasis irrespective of the presence of pathologically positive nodes. Furthermore, only the presence of micrometastasis was independently associated with biochemical recurrence regardless of other factors examined. **Conclusions:** These findings suggest that ~30% of clinically localized prostate cancers shed cancer cells to the pelvic lymph nodes, and that biochemical recurrence after radical prostatectomy could be explained, at least in part, by micrometastases in pelvic lymph nodes.

Pelvic lymph node metastasis has been considered the most important predictive factor of disease recurrence in patients with clinically localized prostate cancer who have undergone radical prostatectomy. Patients with organ-confined prostate cancer have a good prognosis and a low risk of disease recurrence following radical prostatectomy, whereas biochem-

ical recurrence, characterized by an increasing serum prostate-specific antigen (PSA) value, occurs in ~10% of patients in this category (1, 2). Because routine microscopic examination of lymphadenectomy specimens can miss small cancer foci, this finding might partially account for the presence of histologically undetectable micrometastases in the pelvic lymph nodes. In fact, various investigators have shown that higher sensitivity for detecting micrometastatic cancer cells in surgically removed pelvic lymph nodes at radical prostatectomy can be achieved by several molecular and histologic techniques targeting prostate-specific gene expression, including reverse transcriptase-PCR (RT-PCR) and immunohistochemical staining (3-6). To date, however, none of these methods have been introduced into clinical practice due to various limitations, such as a high false-positive rate and complicated procedures. Collectively, these findings suggest that an improved approach for detecting micrometastatic prostate cancer cells in the lymph nodes needs to be identified.

Recently, a real-time detection and quantitative PCR-based assay was developed (7). The advantage of this assay is the

**Authors' Affiliations:** <sup>1</sup>Department of Urology, Kobe University School of Medicine, Kobe, Japan and <sup>2</sup>Department of Urology, Hyogo Medical Center for Adults, Akashi, Japan

Received 12/13/05; revised 5/3/06; accepted 5/15/06.

**Grant support:** Grant-in-Aid from the Ministry of Education, Science, and Culture of Japan.

The costs of publication of this article were defrayed in part by the payment of page charges. This article must therefore be hereby marked *advertisement* in accordance with 18 U.S.C. Section 1734 solely to indicate this fact.

**Requests for reprints:** Hideaki Miyake, Department of Urology, Kobe University School of Medicine, 7-5-1 Kusunoki-cho, Chuo-ku, Kobe 650-0017, Japan. Phone: 81-78382-6155; Fax: 81-78382-6169; E-mail: hideakimiyake@hotmail.com.

©2007 American Association for Cancer Research.

doi:10.1158/1078-0432.CCR-05-2706



specific detection of rare events; that is, sensitivity has been shown to allow for the detection of 10 to 100 pg of RNA from the target gene. Furthermore, it is highly reproducible and quantitative, significantly eliminating the risks of contamination encountered with other types of PCR-based assays, and requires no post-PCR product manipulation. Accordingly, the method has been widely used for accurately detecting occult micrometastatic tumor burden in resected lymph node specimens (8–12). For example, Van Trappen et al. used real-time RT-PCR targeting the cytokeratin 19 gene, and reported that ~50% of early stage cervical cancers shed tumor cells to the pelvic nodes, and the amount of cytokeratin 19 expression was related to the clinicopathologic features (8). To our knowledge, however, there has not been any study analyzing lymph node specimens obtained from patients with prostate cancer using real-time RT-PCR assay in order to clarify the significance of micrometastases in biochemical recurrence after successful radical surgery.

Expression of the PSA and prostate-specific membrane antigen (PSMA) genes is exclusively restricted to prostate epithelial cells (4), and this high specificity made it possible to identify metastatic prostate cancer cells among non-prostate cells. Moreover, these two genes are expressed heterogeneously in prostate epithelial cells (4); thus, simultaneous targeting of these two specific antigens might promote the detection of metastatic prostate cancer cells with a wide phenotypic spectrum. Considering these findings, we did a fully quantitative real-time RT-PCR assay targeted against PSA and PSMA gene expression in 2,215 fresh pelvic lymph nodes obtained from 120 patients with clinically localized prostate cancer, then analyzed the clinical significance of occult micrometastasis of prostate cancer cells to pelvic lymph nodes.

## Patients and Methods

**Surgical specimens.** This study was approved by the research ethics committee of our institution, and informed consent was obtained from all patients at the time of enrollment. Lymph node specimens were obtained from 120 patients with clinically localized prostate cancer who underwent radical retropubic prostatectomy and pelvic lymphadenectomy without neoadjuvant therapies between October 2001 and July 2004. Pelvic lymphadenectomy was done, targeting the obturator fossa and external iliac region by removing all fatty, connective, and lymphatic tissue. Lymph node samples were also available from seven female patients with invasive bladder cancer who underwent radical cystectomy. Each lymph node was bisected. One half was snap-frozen immediately and stored at  $-80^{\circ}\text{C}$  until assessed, and the remainder was fixed in formalin, embedded in paraffin, and stained with H&E for histopathologic examination. In this series, all pathologic examinations were done by a single pathologist according to the Union Internationale Contra Cancrum (tumor-node-metastasis) tumor stage classification (13). Biochemical recurrence was defined as a serum PSA level of  $\geq 0.2$  ng/mL; none of the patients received any additional therapies until their serum PSA levels reached  $\geq 0.4$  ng/mL.

**Real-time RT-PCR assay.** Total RNA was extracted from lymph node specimens using the acid guanidinium isothiocyanate, phenol chloroform method, and 1  $\mu\text{g}$  of each total RNA was reverse-transcribed using an Oligo dT and Superscript preamplification system (Life Technologies, Rockville, MD). To analyze the expression levels of PSA, PSMA, and glyceraldehyde-3-phosphate dehydrogenase (GAPDH) mRNAs, real-time quantitative PCR was done using Sequence Detector (ABI PRISM 7700; PE Applied Biosystems, Foster City, CA). The sequences of primers and probes for these genes were determined by Primer Express

software (PE Applied Biosystems). Selected sequences of forward (F) and reverse (R) primers, and probes are as follows: PSA F, 5' CGTGG-ATTGGTGCTGCAC 3'; PSA R, 5'-TGGGAATGCTTCTCGCACTC-3'; PSA probe, 5'-CCTGTCTCGGATTGTGGGAGGCTG-3'; PSMA F, 5'-TTCTGT-TAAAAGCAGTGCTTCCAT-3'; PSMA R, 5'-CGTATTTTCGAGGGAGAGAA-TAGCTA-3'; PSMA probe, 5'-CACGGCCTCTCTCACGGATTATAAGA-ACACA-3'; GAPDH F, 5'-GAAGGTGAAGTCCGGAGTC-3'; GAPDH R, 5'-GAAGATGGTGATGGGATTTC-3'; GAPDH probe, 5'-CAAGCTCCC-GTTCTCAGCC-3'. The probes used in this study consisted of an oligodeoxynucleotide with a 5' FAM (6-carboxy-fluorescein) reporter dye and 3' TAMRA (6-carboxy-tetramethylrhodamine) quencher dye. Each complementary DNA was analyzed by quantitative PCR in a 50  $\mu\text{L}$  volume using Master Mix (PE Applied Biosystems). The thermal cycling conditions were composed of 50 cycles of amplification consisting of 15 s at  $95^{\circ}\text{C}$  and 1 min at  $60^{\circ}\text{C}$ .

Real-time quantitation was done based on TaqMan assay according to the manufacturer's instruction as described previously (14, 15). After the generation of a real-time amplification plot based on normalized fluorescence signals, the threshold cycle (Ct), which is the fractional cycle number at which the amount of amplified target reached a fixed threshold, was determined. The Ct was then used for kinetic analysis and was proportional to the initial number of target copies in the sample. The starting quantity of a sample was calculated after comparison to the Cts of a serial dilution of a positive control, human prostate cancer LNCaP cells (American Type Culture Collection, Rockville, MD). All serial dilutions were carried out in duplicate, and the reactions to generate standard curves were repeated twice (each time in triplicate). All clinical specimens were also analyzed in triplicate and the mean values were used for quantification. The coefficient of variation for triplicate reactions was  $<10\%$ , and the coefficient of variation between assays was also  $<10\%$ . In this series, except for samples in which PSA and/or PSMA were not amplified, the ranges of Ct values for PSA and PSMA were as follows: PSA, 17.2 to 43.4; PSMA, 13.3 to 41.1.

Both the precise amount and quality of total RNA added to each reaction mix are extremely difficult to assess; therefore, transcripts of the GAPDH gene were quantified as an internal reference according to a quantitative PCR assay. The quantification value of PSA or PSMA mRNA was described as each value relative to GAPDH mRNA. To exclude false positives, we used the mean relative mRNA value plus 2 SDs of PSA or PSMA mRNA expression in 148 lymph nodes from female patients with bladder cancer as the cutoff value for PSA or PSMA, respectively, and values above the cutoff value for PSA or PSMA mRNA were defined as PSA- or PSMA mRNA-positive, respectively. In this study, we regarded specimens in which PSA and/or PSMA mRNA were positive as proof of the "presence of micrometastasis."

**Immunohistochemical staining.** In cases diagnosed as having micrometastases according to real-time RT-PCR, despite the lack of positive findings on routine pathologic examinations, sections adjunct to the site of the original sections for H&E staining were cut from the original formalin-fixed, paraffin-embedded blocks, and examined to determine whether occult foci of prostate cancer cells were present by immunohistochemical staining with a monoclonal antibody against PSA (Dako, Carpinteria, CA) using standard immunohistochemical techniques as reported previously (16). After staining, the sections were counterstained with hematoxylin. All slides were reviewed by the same pathologist without knowledge of any clinicopathologic data, as described above.

**Statistical analysis.** Differences between the two groups were compared using the  $\chi^2$  test, unpaired *t* test, or Mann-Whitney *U* test. The biochemical recurrence-free survival rates were calculated by the Kaplan-Meier method, and the difference was determined by log rank test. Forward stepwise logistic regression analysis was used to determine the association between several variables and biochemical recurrence. The significance of several factors in the time to biochemical recurrence was assessed by the Cox proportional hazards regression model. All statistical calculations were done using StatView 5.0 software

**Table 1.** Outcomes of histologic examination and real-time RT-PCR assay

	Group A	Group B	Group C
No. of patients	11	32	77
No. of dissected lymph nodes	201	619	1,395
Histologic examination			
No. of positive patients	11	0	0
No. of positive lymph nodes	29	0	0
Real-time RT-PCR assay for PSA			
No. of positive patients	11	23	0
No. of positive lymph nodes	51	84	0
Real-time RT-PCR assay for PSMA			
No. of positive patients	11	29	0
No. of positive lymph nodes	71	112	0
Micrometastasis			
No. of positive patients	11	32	0
No. of positive lymph nodes	82	143	0

NOTE: Group A, patients with histologically confirmed lymph node metastases; group B, patients with micrometastases despite the lack of histologic evidence indicating nodal involvement; and group C, patients without any findings of lymph node metastases.

(Abacus Concepts, Inc., Berkeley, CA), and  $P < 0.05$  was considered significant.

**Results**

The expression of GAPDH mRNA in all lymph node specimens was confirmed. In 148 lymph nodes from seven female patients with bladder cancer, the mean values of relative PSA and PSMA mRNAs expression plus 2 SDs were 2.8 and 4.9, respectively, and these values were used as cutoff points for the positive expression of PSA and PSMA mRNA in lymph nodes from patients with prostate cancer in the subsequent study. Real-time RT-PCR assays in 2,215 pelvic lymph nodes from patients with clinically localized prostate cancer detected various amounts of relative expression levels of PSA and PSMA mRNAs (PSA: mean, 2.5; median, 0.6; range, 0-193; PSMA: mean, 4.4; median, 1.2; range, 0-792).

Twenty-nine of the 201 lymph nodes from 11 patients with prostate cancer showed histopathologic evidence of

metastatic involvement, and real-time RT-PCR confirmed the expression of PSA and PSMA mRNAs in 29 and 28 nodes, respectively. In these 11 patients, positive PSA and/or PSMA mRNA expression was detected in an additional 53 histologically uninvolved lymph nodes; thus, a total of 82 lymph nodes were diagnosed as having occult micrometastases using real-time RT-PCR assay. Of the 2,014 nodes from the remaining 109 patients without histologic evidence of pelvic lymph node metastases, positive PSA and PSMA mRNA expression were detected in 84 nodes from 23 patients and 112 nodes from 29 patients, respectively. Among these, 53 nodes from 20 patients were judged positive for both PSA and PSMA mRNAs expression; therefore, a total of 32 patients were regarded as having micrometastases to pelvic lymph nodes. The relative expression levels of PSA and PSMA mRNAs in 225 nodes considered positive for micrometastases were as follows: (PSA) mean, 17.2; median, 15.1; range 1.9 to 193; (PSMA) mean, 32.4; median, 24.4; range, 3.1 to 792. These outcomes are summarized in Table 1 by dividing 120 patients into the following three groups: 11 with histologically detected lymph node metastases (group A), 32 with micrometastases despite the lack of histologic evidence indicating nodal involvement (group B), and the remaining 77 without any findings of lymph node metastases on histologic and real-time RT-PCR analyses (group C).

The incidence of micrometastases according to anatomic location was analyzed. Similar metastatic patterns of prostate cancer cells to the external iliac region and obturator fossa were observed between groups A and B, irrespective of the presence of histologically confirmed nodal involvement. We further compared clinicopathologic features among these three groups. As shown in Table 2, despite the absence of significant differences between groups A and B in several of the factors examined, preoperative serum PSA, pathologic stage, Gleason score, and tumor volume in groups A and B were significantly greater than those in group C.

The median follow-up period of the 120 patients included in this study was 38 months (range, 15-48 months). In this series, biochemical recurrence occurred in 8, 17, and 7 patients in groups A, B, and C, respectively (Table 3). The median intervals between radical prostatectomy and biochemical recurrence in groups A, B, and C were 6, 11, and 17 months, respectively. As

**Table 2.** Comparison of conventional prognostic indicators according to lymph node metastases detected by histologic examination and real-time RT-PCR assay

	Groups			P		
	A	B	C	A vs. B	B vs. C	C vs. A
No. of patients	11	32	77			
Preoperative serum PSA (ng/mL)*	25.3 ± 24.7	20.2 ± 18.7	9.8 ± 6.9	0.48	<0.0001	<0.0001
Pathologic stage (no. of patients)				0.23	0.0008	<0.0001
pT <sub>2</sub>	1	11	55			
pT <sub>3</sub>	9	20	22			
pT <sub>4</sub>	1	1	0			
Gleason score*	8.1 ± 4.1	7.5 ± 3.9	6.1 ± 2.9	0.67	0.041	0.046
Tumor volume (cm <sup>3</sup> )*	2.5 ± 1.7	2.0 ± 1.4	0.92 ± 0.65	0.34	<0.0001	<0.0001

NOTE: Group A, patients with histologically confirmed lymph node metastases; group B, patients with micrometastases despite the lack of histologic evidence indicating nodal involvement; group C, patients without any findings of lymph node metastases.  
\*Data are presented as mean ± SD.

**Table 3.** Incidence of biochemical recurrence according to lymph node metastases detected by histologic examination and real-time RT-PCR assay

	Groups			P		
	A	B	C	A vs. B	B vs. C	C vs. A
No. of patients	11	32	77			
No. of patients with biochemical recurrence (%)	8 (72.7)	17 (53.1)	7 (9.1)	0.26	<0.0001	<0.0001
Mean time to biochemical recurrence after prostatectomy (mo)*	9.5 ± 9.9	14.9 ± 7.6	21.0 ± 9.9	0.86	0.032	0.0004
Pathologically organ-confined disease						
No. of patients with biochemical recurrence/total no. of patients	0/0	4/11	2/55	—	0.0006	—
Pathologically extraprostatic disease						
No. of patients with biochemical recurrence/total no. of patients	8/11	13/21	5/22	0.54	0.092	0.0056

NOTE: Group A, patients with histologically confirmed lymph node metastases; group B, patients with micrometastases despite the lack of histologic evidence indicating nodal involvement; group C, patients without any findings of lymph node metastases.  
\*Data are presented as mean ± SD.

shown in Fig. 1, biochemical recurrence-free survival rates in groups A and B were significantly lower than that in group C. However, there was no significant association between the number of positive nodes for micrometastases as well as quantitative values of PSA and PSMA expression with biochemical recurrence (data not shown). In addition, of the 66 patients with pathologically organ-confined disease, only 6 developed biochemical recurrence, among whom 4 were diagnosed as having micrometastases in the pelvic lymph nodes (Table 3).

To evaluate the association between several clinicopathologic factors with biochemical recurrence, multivariate analysis using a stepwise logistic regression model was done. As shown in Table 4, only the presence of micrometastasis was independently related to whether or not biochemical recurrence occurred. Furthermore, multivariate analysis using the Cox regression hazard model showed that only the presence of micrometastasis was independently associated with biochemical recurrence-free survival, irrespective of other factors examined in this study (Table 4).

To further confirm the presence of micrometastatic diseases in pelvic lymph nodes, immunohistochemical stainings were done with a monoclonal antibody against PSA in 143 lymph nodes from 32 patients diagnosed as having micrometastases using real-time RT-PCR assays (despite the lack of pathologic evidence of nodal involvement). Sixty-one of the 143 lymph nodes (from 17 patients) were evidently stained with PSA antibody. Representative results are shown in Fig. 2.

**Discussion**

Lymph node metastasis is the most useful factor predicting poor prognosis in patients undergoing radical prostatectomy for clinically localized prostate cancer. However, ~30% of such patients without evidence of pathologic nodal involvement will develop biochemical disease recurrence (1, 2). Although the etiology of biochemical disease recurrence following radical

prostatectomy is likely multifactorial, a significant proportion of these recurrences might be due to occult metastases to pelvic lymph nodes undetected by routine pathologic examinations. Several investigators have assessed whether microscopic foci of prostate cancer cells are present in histologically uninvolved pelvic nodes using molecular and histochemical approaches (3–6), but the clinical significance of micrometastases in pelvic nodes remains controversial. Because accurate staging of prostate cancer facilitates the prediction of therapeutic outcomes and appropriate tailoring of adjuvant therapies to the individual patient, we investigated PSA and PSMA mRNA expression in 2,215 pelvic lymph nodes dissected at radical prostatectomy from 120 patients with clinically localized prostate cancer using quantitative real-time RT-PCR assay, evaluated the sensitivity of this assay for detecting occult lymph

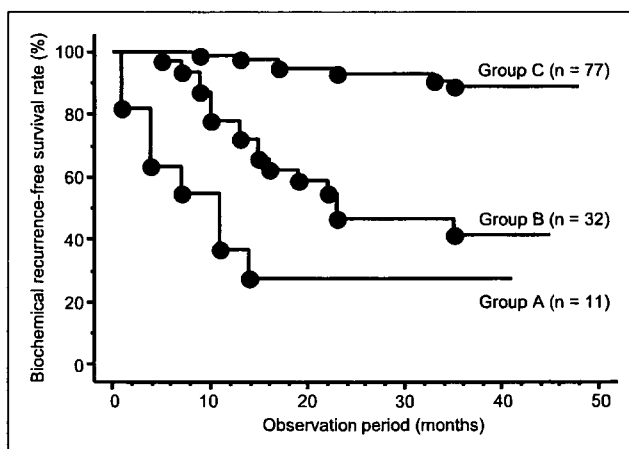


**Fig. 1.** Comparison of biochemical recurrence-free survival rates in groups A, B, and C using the Kaplan-Meier method. The biochemical recurrence-free survival rates in groups A and B were significantly lower than that in group C ( $P = 0.059$ , group A versus group B;  $P < 0.0001$ , group B versus group C;  $P < 0.0001$ , group C versus group A using the log-rank test).

**Table 4.** Multivariate analyses of various factors in relation to biochemical recurrence

Variables	P value	
	Stepwise logistic regression model	Cox proportional hazards regression model
Serum PSA, ng/mL (<10 vs. ≥10)	0.55	0.61
Pathologic stage (pT <sub>2</sub> vs. pT <sub>3</sub> or pT <sub>4</sub> )	0.23	0.51
Gleason score (6 or 7 vs. 8, 9, or 10)	0.14	0.10
Tumor volume, cm <sup>3</sup> (<1.0 vs. ≥1.0)	0.44	0.33
Micrometastasis (negative vs. positive)	0.040	0.032

node metastases, and analyzed various clinicopathologic factors according to the assay findings.

In this series, standard pelvic lymphadenectomy targeting the external iliac region and obturator fossa for all 120 patients was done, and the mean number of lymph nodes removed at radical prostatectomy in these patients was 18.5. Based on an autopsy study, approximately 20 lymph nodes have been shown to serve as a guideline for optimal and representative pelvic lymph node dissection (17), suggesting that the procedure for pelvic lymphadenectomy done in this study, which met this requirement, would be suitable. We also examined 148 pelvic lymph nodes obtained from seven female patients undergoing radical cystectomy for invasive bladder cancer to determine the appropriate cutoff points for the positive expression of PSA and PSMA mRNAs on real-time RT-PCR. Although it is a potentially crucial point to reduce the false positivity of real-time RT-PCR, it is usually difficult to establish cutoff points on this assay for diseases lacking specific markers. However, PSA and PSMA gene expressions are highly restricted to prostate epithelial cells (4); that is, although it is inevitable to detect extremely low levels of PSA and PSMA expressions considering the principle of this assay, lymph nodes from females theoretically do not express these genes, indicating that the cutoff points used in this study were properly determined. Furthermore, in order to avoid underestimating the significance of micrometastases of prostate cancer cells, the expression levels of both PSA and PSMA mRNAs in each node, which were shown to be heterogeneously expressed in prostate cancers (4), were measured, and nodes diagnosed as positively expressing PSA and/or PSMA mRNA were judged to be the presence of micrometastatic cancer foci. Collectively, these findings suggest that the present study was carried out under ideal conditions, which contributes to the reliability of the current outcomes.

We diagnosed the presence of occult micrometastasis in 225 lymph nodes from 43 patients using real-time RT-PCR assay, including 29 histologically involved nodes from 11 patients. This proportion of micrometastases to pelvic lymph nodes was significantly high compared with that reported in previous studies evaluated by RT-PCR (3, 4), suggesting that the real-time RT-PCR assay used in this study was more sensitive than conventional RT-PCR. In addition, the differences in the procedures between real-time RT-PCR and conventional RT-PCR contribute to the enhanced specificity; that is, it does not require post-PCR manipulation, and quantitation and calculation are all automated. In fact, immunohistochemical staining with PSA antibody detected micrometastatic cancer foci in approximately half of the pelvic nodes diagnosed as positive for micrometastasis despite the lack of histologic findings.

Characterization of clinicopathologic features according to nodal status showed that there were no significant differences in several conventional prognostic factors between patients with histologically detected nodal involvement and those with nodes positive for micrometastases despite the lack of histologically positive findings. Anatomic locations of micrometastatic nodes were also similar between these two patient groups. In addition, the proportion of patients positive for micrometastases was closely related to several poor prognostic indicators (data not shown). These findings strongly suggest that even with the lack of histologic confirmation, some of the

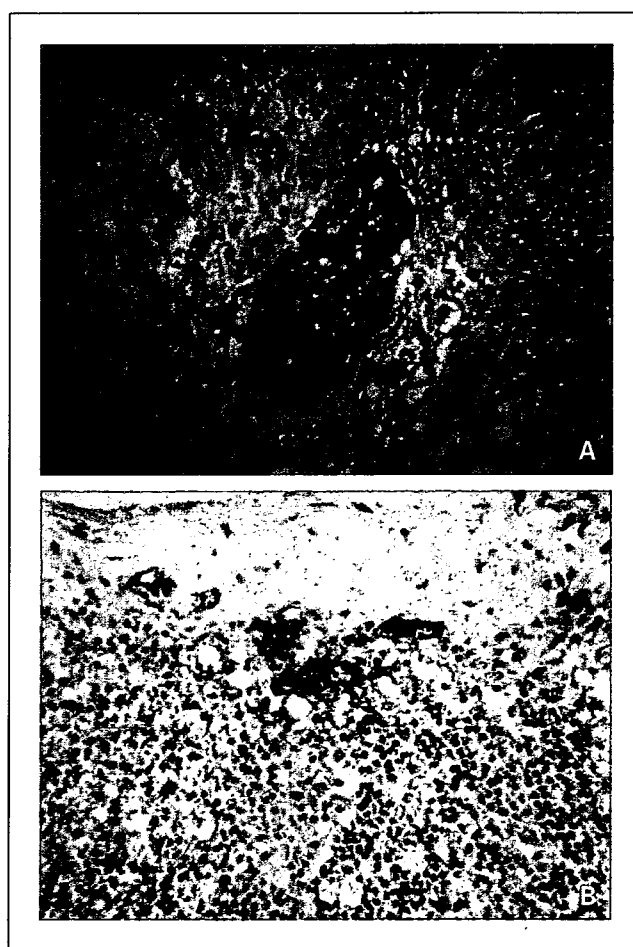


**Fig. 2.** Representative results of immunohistochemically detected micrometastatic cancer foci using a monoclonal antibody against PSA in histologically uninvolved lymph node specimens (A and B).

micrometastatic diseases diagnosed by the current real-time RT-PCR assay have biological characteristics similar to those of histologically positive nodal diseases. This hypothesis was supported by the incidence of biochemical recurrence following radical prostatectomy. Although the follow-up period of this study was too short to draw conclusions concerning the prognosis, there were no significant differences in the incidence of biochemical recurrence between these two groups. In addition, biochemical recurrence in four patients with pathologically organ-confined disease (diagnosed as positive for micrometastases) also supports this hypothesis. Furthermore, the presence of micrometastasis was independently associated with whether or not biochemical recurrence occurred—as well as the time to biochemical recurrence. Although longer follow-up periods are absolutely necessary to draw a definitive conclusion, the present findings suggest that some micrometastases in pelvic lymph nodes may, at least in part, contribute to the development of biochemical recurrence following radical prostatectomy.

To further address the significance of micrometastases in prostate cancer, several problems should be elucidated. For example, it would be of interest to investigate whether histologically undetectable or dormant micrometastatic disease in the lymphatic system will always progress to clinically significant recurrence after variable disease-free recurrence. If not, it will be necessary to develop a diagnostic system differen-

tiating significant micrometastatic diseases from insignificant disease. Recent studies have reported the possible effect of lymphadenectomy on the survival of patients with pathologically confirmed positive nodes who underwent radical prostatectomy (18, 19). If there is a survival benefit in pelvic lymph node dissection for such patients, it would be interesting to evaluate whether removing micrometastatic nodes affects the prognosis. Recently, several investigators showed the usefulness of novel approaches for detecting occult prostate cancer metastases in lymph nodes (20, 21). For example, Shariat et al. reported that a splice variant-specific RT-PCR targeting the human glandular kallikrein gene can detect biologically and clinically significant micrometastases of prostate cancer in histopathologically normal lymph nodes (21). The assessment of these issues may facilitate the determination of a more appropriate procedure for lymphadenectomy considering the findings on molecular staging.

In conclusion, the results of this study showed the usefulness of quantitative real-time RT-PCR targeting the expression of PSA and PSMA genes for identifying micrometastatic tumor foci in pelvic lymph nodes from clinically localized prostate cancer at radical prostatectomy. Although longer follow-up periods are absolutely necessary to draw a definitive conclusion, the present findings suggest that some micrometastases in pelvic lymph nodes may, at least in part, contribute to the development of biochemical recurrence after radical prostatectomy.

## References

- Walsh PC, Partin AW, Epstein JI. Cancer control and quality of life following anatomical radical retropubic prostatectomy: results at 10 years. *J Urol* 1994;152:1831–6.
- Catalona WJ, Smith DS. Cancer recurrence and survival rates after anatomic radical retropubic prostatectomy for prostate cancer: intermediate-term results. *J Urol* 1998;160:2428–34.
- Okegawa T, Nutahara K, Higashihara E. Detection of micrometastatic prostate cancer cells in the lymph nodes by reverse transcriptase polymerase chain reaction is predictive of biochemical recurrence in pathological stage T2 prostate cancer. *J Urol* 2000;163:1183–8.
- Potter SR, Mangold LA, Shue MJ, et al. Molecular and immunohistochemical staging of men with seminal vesicle invasion and negative pelvic lymph nodes at radical prostatectomy. *Cancer* 2000;89:2577–86.
- Ferrari AC, Stone NN, Eyer JN, et al. Prospective analysis of prostate-specific markers in pelvic lymph nodes of patients with high-risk prostate cancer. *J Natl Cancer Inst* 1997;89:1498–504.
- Wawroschek F, Wagner T, Hamm M, et al. The influence of serial sections, immunohistochemistry, and extension of pelvic lymph node dissection on the lymph node status in clinically localized prostate cancer. *Eur Urol* 2003;43:132–7.
- Gibson UE, Heid CA, Williams PM. A novel method for real time quantitative RT-PCR. *Genome Res* 1996;6:995–1001.
- Van Trappen PO, Gyselman VG, Lowe DG, et al. Molecular quantification and mapping of lymph-node micrometastases in cervical cancer. *Lancet* 2001;357:15–20.
- Mrras M, Mikhitarian K, Walters C, et al. Quantitative real-time RT-PCR detection of breast cancer micrometastasis using a multigene marker panel. *Int J Cancer* 2001;93:162–71.
- Yoshioka S, Fujiwara Y, Sugita Y, et al. Real-time reverse transcriptase-polymerase chain reaction for intraoperative diagnosis of lymph node micrometastasis: clinical application for cervical lymph node dissection in esophageal cancers. *Surgery* 2002;132:34–40.
- Kubota K, Nakanishi H, Hiki N, et al. Quantitative detection of micrometastases in the lymph nodes of gastric cancer patients with real-time RT-PCR: a comparative study with immunohistochemistry. *Int J Cancer* 2003;105:136–43.
- Inokuchi M, Ninomiya I, Tsugawa K, Terada I, Miwa K. Quantitative evaluation of metastases in axillary lymph nodes of breast cancer. *Br J Cancer* 2003;89:1750–6.
- Sobin LH, Wittekind CH, editors. TNM classification of malignant tumors. 5th ed. New York: Wiley-Liss; 1997.
- Das H, Koizumi T, Sugimoto T, et al. Quantitation of Fas and Fas ligand gene expression in human ovarian, cervical and endometrial carcinomas using real-time quantitative RT-PCR. *Br J Cancer* 2000;82:1682–8.
- Kurahashi T, Hara I, Oka N, Kamidono S, Eto H, Miyake H. Detection of micrometastases in pelvic lymph nodes in patients undergoing radical cystectomy for locally invasive bladder cancer by real-time reverse transcriptase-PCR for cytokeratin 19 and uroplakin II. *Clin Cancer Res* 2005;11:3773–7.
- Kurahashi T, Muramaki M, Yamanaka K, Hara I, Miyake H. Expression of the secreted form of clusterin protein in renal cell carcinoma as a predictor of disease extension. *BJU Int* 2005;96:895–9.
- Weingartner K, Ramaswamy A, Bittinger A, et al. Anatomical basis for pelvic lymphadenectomy in prostate cancer: results of an autopsy study and implications for the clinic. *J Urol* 1996;156:1969–73.
- Bader P, Burkhard FC, Markwalder R, et al. Disease progression and survival of patients with positive lymph nodes after radical prostatectomy. Is there a chance of cure? *J Urol* 2003;169:849–54.
- Cheng L, Zincke H, Blute ML, et al. Risk of prostate carcinoma death in patients with lymph node metastasis. *Cancer* 2001;91:66–73.
- Haas CJ, Wagner T, Wawroschek F, Arnholt H. Combined application of RT-PCR and immunohistochemistry on paraffin embedded sentinel lymph nodes of prostate cancer patients. *Pathol Res Pract* 2005;200:763–70.
- Shariat SF, Kattan MW, Erdamar S, et al. Detection of clinically significant, occult prostate cancer metastases in lymph nodes using a splice variant-specific rt-PCR assay for human glandular kallikrein. *J Clin Oncol* 2003;21:1223–31.

## Exploration of Target Molecules for Prostate Cancer Gene Therapy

Kazuhiro Suzuki,<sup>1,2</sup> Kiminori Nakamura,<sup>1</sup> Kazunori Kato,<sup>1</sup>  
Hirofumi Hamada,<sup>1</sup> and Taiji Tsukamoto<sup>2\*</sup>

<sup>1</sup>Department of Molecular Medicine, Sapporo Medical University School of Medicine, Sapporo, Japan

<sup>2</sup>Department of Urology, Sapporo Medical University School of Medicine, Sapporo, Japan

**BACKGROUND.** Focusing on Adv-FZ33, a modified adenovirus in which a synthetic 33-amino-acid immunoglobulin G-binding domain was inserted into the adenoviral fiber protein, we tried to identify suitable target molecules for prostate cancer-specific gene therapy.

**METHODS.** Hybridomas were established from mice immunized with prostate cancer cell lines. The hybridomas were screened using Adv-FZ33 to create monoclonal antibodies (mAbs) that induced high gene transfer efficiency for PC-3 cells. Furthermore, we identified target antigens of the mAbs by immunoprecipitation and mass spectrometry, and investigated the expression of target molecules by flow cytometry and immunocytochemistry.

**RESULTS.** Using Adv-FZ33, we established four different mouse mAbs that increased transduction efficiency for PC-3. The target antigens identified were Ep-CAM, CD155, HAI-1, and Na,K-ATPase  $\beta$ 1. These antigens were expressed in several cancer cell lines, including prostate cancer. Human prostatic myofibroblast cells lacked expression of Ep-CAM and HAI-1.

**CONCLUSIONS.** We established anti-Ep-CAM mAb and anti-HAI-1 mAbs. Gene transduction via Ep-CAM and HAI-1 may be a novel strategy for treatment of prostate cancer. *Prostate* 67: 1163–1173, 2007. © 2007 Wiley-Liss, Inc.

**KEY WORDS:** gene therapy; modified adenovirus vector; prostate cancer; monoclonal antibody

### INTRODUCTION

Prostate cancer is the most common cancer in the West and the second leading cause of male cancer-related death [1]. Advanced androgen-insensitive prostate cancer exhibits little or no response to conventional therapies [2]. Thus, gene therapy is anticipated as an alternative treatment for this type of disease [3].

Adenoviral vectors are commonly used in gene therapy. This is due to their ability to produce high titers and infect various cell types [4]. Genes are transferred to target cells via the Coxsackie adenovirus receptor (CAR), which is a cell-surface receptor required for adenovirus attachment [5]. However, because CAR is widely expressed on normal cells, its lack of specificity is still an obstacle for its clinical application in cancer-gene therapy. In this context, we focused on the function of fiber Z33 type adenovirus (Adv-FZ33). This adenovirus has a synthetic 33-amino-

acid immunoglobulin G (IgG)-binding domain (Z33) derived from staphylococcal protein A inserted into the virus having fiber protein [6]. This modified fiber binds IgG with high affinity and allows an antibody to redirect the vector to a new target molecule on the cell surface.

In this study, we established hybridomas from mice splenocytes immunized with prostate cancer cell lines. Then we selected from them monoclonal antibodies

Grant sponsor: Stiftelsen Japanese-Swedish Research Foundation; Grant sponsor: Cancer Research from the Ministry of Health and Welfare of Japan; Grant sponsor: Ministry of Education, Culture, Sports, Science and Technology.

\*Correspondence to: Taiji Tsukamoto, MD, Department of Urology, Sapporo Medical University School of Medicine, S-1, W-16, Chuo-Ku, Sapporo 060-8543, Japan. E-mail: taijit@sapmed.ac.jp

Received 12 January 2007; Accepted 4 April 2007

DOI 10.1002/pros.20613

Published online 21 May 2007 in Wiley InterScience (www.interscience.wiley.com).

(mAbs) that increased transduction efficiency by bridging Adv-FZ33 with prostate cancer.

**MATERIALS AND METHODS**

**Cell Lines**

We used human prostate cancer cell lines (PC-3, LNCaP, and DU145), a human renal cell carcinoma cell line (Caki-1), a bladder cancer cell line (T24), an ovarian cancer cell line (SKOV-3), normal dermal fibroblasts (PDF), normal prostate myofibroblasts (PrMFB), human embryonic kidney cells (293 T), and mouse myeloma (P3U1). These cell lines were purchased from American Type Culture collection (Manassas, VA). PrMFB was established in our department [7]. Cells were cultured in RPMI-1640 supplemented with 10% fetal calf serum, 1% non-essential amino acids, 1 mm sodium pyruvate, and 1% streptomycin/penicillin solution.

**Adenoviral Vectors**

We generated adenoviral vectors containing the IgG-binding Z33 motif from Staphylococcal protein A at the HI-loop of the adenovirus type 5 (Ad5) fiber knob, and designated it Adv-FZ33 (represented in Fig. 1A). Details of Adv-FZ33 construction were described in a previous study [8].

**Production and Screening of Hybridomas**

Screening protocol for targeting mAbs is represented in Figure 1C. A Balb/c mouse was injected intraperitoneally with a mixture of PC-3, LNCaP, and DU145 cells (total:  $2 \times 10^6$ ) every 14 days. Three days after the 5th injection, the mouse was sacrificed and  $1 \times 10^8$  mouse splenocytes were fused with  $2 \times 10^7$  P3U1 cells using polyethylene glycol (PEG). When hybridomas grew to about 50% confluence, culture supernatants were tested for antibody activity. PC-3

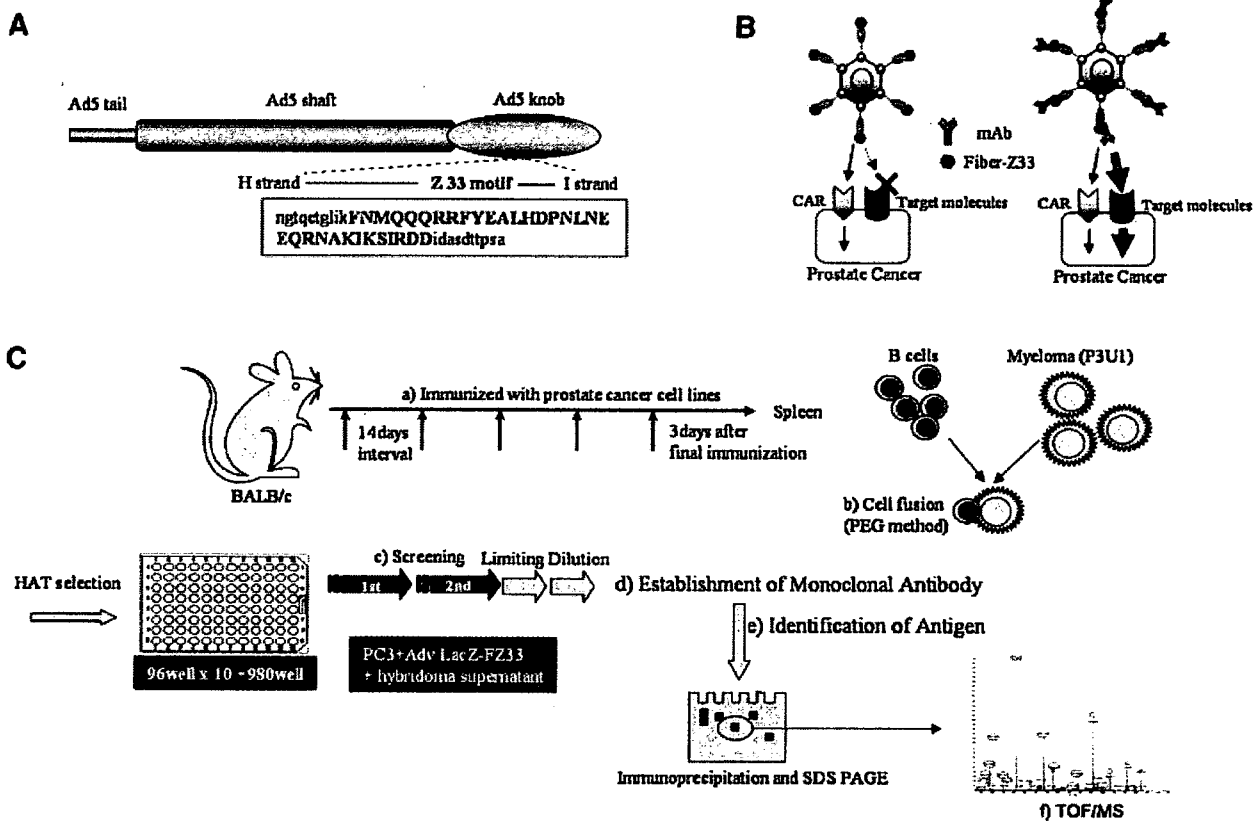


**Fig. 1.** Schematic representation of Adv-FZ33 and procedure for the establishment of cancer-targeting antibodies. **A:** Z33-modified Ad5 fiber A synthetic 33-amino acid IgG-binding domain (Z33), derived from staphylococcal protein A, was inserted into the HI loop of knob protein. **B:** Targeting with Adv-FZ33 Adv-FZ33 binds immunoglobulins and allows an antibody to redirect the vector to a new target molecule on the cell surface. Our Adv-FZ33 had intact CAR-binding structure and retained CAR-binding ability. **C:** Methods for establishment of novel cancer-targeting antibodies using Adv LacZ-FZ33. (a) Immunization with prostate cancer cell lines. (b) Cell fusion with PEG method. (c) Screening and limiting dilution. (d) Establishment of monoclonal antibody. (e) Identification of antigen by immunoprecipitation and SDS-PAGE. (f) Detection of molecule by mass spectrometry.

cells were prepared in 96-well microplates. After the removal of the culture medium, supernatants were added to each well and incubated for 1 hr at 4°C, after which supernatants were removed and microplates were washed with PBS. Adv-FZ33 inserted LacZ reporter gene (Adv LacZ -FZ33) prepared in FBS-free RPMI-1640 at a multiplicity of infection (MOI) of 1,000 vp/cell was added to each well and incubated for 1 hr at 4°C. Then microplates were washed twice with PBS and incubated at 37°C in a 5% CO<sub>2</sub> incubator. Twenty-four hours after infection, chemiluminescent β-Gal reporter gene assays (Roche Diagnostics, Mannheim, Germany) were performed according to the company's recommendations. Hybridomas that showed high β-Gal activity were picked through first and second screenings and cloned by twice limiting dilution. These hybridomas were injected into nude mice intraperitoneally. The mouse monoclonal antibody was purified from ascites of nude mice using protein G sepharose beads (Amersham Bioscience, Uppsala, Sweden). A commercial kit (Roche Diagnostics) was used to detect the isotypes of antibodies.

#### Identification of Target Molecules

**Immunoprecipitation of biotinylated protein and detection of molecular weight.** First,  $2 \times 10^6$  PC-3 cells were prepared and the cell surface was biotinylated (PIERCE, Rockford, IL). Membranes were solubilized on ice for 30 min in 1 ml of buffer containing 1% NP40, 50 mM Tris-HCl, pH 7.6, 150 mM NaCl, and protease inhibitor cocktail (Roche Diagnostics). Samples were cleared of nuclear fragments by centrifugation for 20 min at 15,000g at 4°C, then mixed with protein G sepharose beads and incubated for 2 hr at 4°C, after which the beads were centrifuged to remove non-specifically bound proteins. Five μg of the mAbs established in this study and control mouse IgG (eBioscience, San Diego, CA) were added to the supernatant of each sample and allowed to incubate for 2 hr at 4°C. The immunocomplexes were precipitated by addition of protein G sepharose beads to each sample and incubated for 2 hr at 4°C. The supernatant was discarded and the beads were washed six times with solubilization buffer. Immunocomplexes binding with beads were boiled for 5 min in 20 μl of SDS sample buffer containing 5% 2-mercaptethanol. Samples were separated using 5–20% gradient polyacrylamide gels (BioRad, Hercules, CA) and transferred onto nitrocellulose membranes (Millipore, MA). After blocking with 5% milk in TBS consisting of 10 mM Tris-HCl (pH 7.5), 150 mM sodium chloride, and 0.05% Tween-20, the membranes were incubated for 1 hr at room temperature with avidin-horseradish peroxidase (dilution

1:2,000; Amersham Bioscience, Buckinghamshire, England). Detection was carried out by enhanced chemiluminescence (Amersham Bioscience) according to the manufacturer's instructions.

**Silver stain and mass spectrometry.** For this procedure,  $1 \times 10^9$  PC-3 cells were solubilized in 40 ml of buffer as described above. After the removal of nuclear fragments by centrifugation, samples were mixed with protein G sepharose beads and incubated overnight at 4°C to remove non-specifically bound proteins. Five micrograms of the mAbs established in this study and control mIgG1 were added to the supernatant of each sample and allowed to incubate for 2 hr at 4°C. The immunocomplex was precipitated by addition of protein G sepharose beads to each sample and incubated for 2 hr at 4°C. Samples were separated by SDS-PAGE as described above. The polyacrylamide gel was stained using a Silver Stain kit (Wako Pure Chemical Industries, Ltd, Osaka, Japan) according to the company's recommendations. Specifically stained protein bands were extracted from the gel, digested by trypsin, and analyzed by oMALDI-Qq-TOF MS/MS QSTAR Pulsari (Applied Biosystems Japan Ltd, Tokyo, Japan).

**Confirmation of results of mass spectrometry.** The cDNAs of target molecules identified by mass spectrometry were synthesized by reverse transcription or obtained from Open Biosystems, Inc. (Huntsville, AL). Some cDNAs were ligated into the expression vector with pTarget vector (Promega, Madison, WI) or pcDNA3.1(+) vector (Invitrogen, Carlsbad, CA). cDNA was transfected into 293 T cells or CHO cells using Lipofect AMINE Plus reagent (Invitrogen). Forty-eight hours after transfection, transfected cells were washed and then suspended in staining medium (2% FBS/PBS) containing saturating amounts of mAbs established in this study and negative control IgG1 (MOPC-21, BD PharMingen, San Diego, CA) as controls. The reactivity of each mAb was analyzed by flow cytometry using a FACS-Calibur<sup>®</sup> (Becton Dickinson, San Jose, CA).

#### Transduction Efficiency in PC-3

**Flow cytometric analysis.** To examine transduction efficiency using Adv-FZ33 with established mAbs, PC-3 cells were prepared in six-well plates at the concentration of  $1 \times 10^5$  cells/well. After removal of the culture medium, FBS-free RPMI-1640 containing the mAbs created in this study at a concentration of 2 μg/ml was added to each well and incubated for 1 hr at 4°C. Adv-FZ33 inserted the DNA fragment encoding



the enhanced green fluorescence protein (Adv EGFP - FZ33) prepared in FBS-free RPMI-1640 at the MOI of 1,000 vp/cell was added to each well and incubated for 1 hr at 4°C. Then the wells were washed twice with PBS and incubated at 37°C in a 5% CO<sub>2</sub> incubator. Twenty-four hours after infection, cells were collected and their transduction efficiencies were analyzed by flow cytometry using a FACS-Calibur<sup>®</sup>.

**Chemiluminescent  $\beta$ -Gal reporter gene assay.** PC-3 cells were prepared in 96-well plates at the concentration of  $5 \times 10^3$  cells/well and divided into five groups by the concentration of the mAbs and control IgG1, that is 0.001, 0.01, 0.1, 1.0, and 10  $\mu$ g/ml. After removal of the culture medium, 50  $\mu$ l of FBS-free RPMI-1640 at the concentrations of the mAb described above was added to each well and incubated 1 hr at 4°C. Medium was removed and microplates were washed with PBS. Fifty microliters of Adv LacZ-FZ33 at MOI of 1,000 vp/cell prepared in FBS-free RPMI-1640 was added to each well and incubated for 1 hr at 4°C. The microplates were then washed twice with PBS and incubated at 37°C in a 5% CO<sub>2</sub> incubator. Twenty-four hours after infection, chemiluminescent  $\beta$ -Gal reporter gene assays were performed. Furthermore, we compared transduction efficiency of Adv-FZ33 with wild type adenovirus (Ad5). The concentration of virus was divided into 30, 100, 300, 1,000, 3,000, and 10,000 vp/cell. The concentration of mAb and control IgG1 was 1  $\mu$ g/ml.

#### Distribution of Target Antigens

**Flow cytometric analysis.** The reactivity of the mAbs with human cell lines (PC-3, LNCaP, DU145, Caki-1, T24, SKOV-3, PDF, and PrMFB) was analyzed by flow cytometry. Cells in the logarithmic growth phase were trypsinized and washed. A cell pellet containing  $1 \times 10^5$  cells was suspended in staining medium (2% FBS/PBS) containing 2  $\mu$ g of mAb or isotype control IgG as controls for 60 min at 4°C in the dark. After three rinses with PBS, cells were incubated with a fluorescein isothiocyanate (FITC)-conjugated rabbit anti-mouse Ig antibody (diluted 1:100) (TAGO, Inc., Burlingame, CA) for 45 min at 4°C. The cell suspension obtained was washed three times with PBS and then analyzed by flow cytometry.

**Immunohistochemistry.** Study specimens of 30 patients were selected from the clinical pathology archives of the Sapporo Medical University Hospital. They included 30 specimens consisting of 13 needle-core biopsies, 14 prostatectomies, and 3 cystoprostatectomies obtained between 2001 and 2002. All H&E-stained slides were reviewed and the respective

diagnoses were confirmed. All of these specimens included prostatic adenocarcinoma (22 patients with Gleason scores of 5–8, and 8 with Gleason scores of 9).

Immunohistochemistry with mAbs created in this study was performed on 5- $\mu$ m thick, formalin-fixed paraffin-embedded tissue sections mounted on poly L-lysine-coated slides. The concentration of the mAb as the primary antibody was 5  $\mu$ g/ml. Details of immunohistochemistry methods were described in a previous study [9].

## RESULTS

### Establishment of Hybridomas and Mouse Monoclonal Antibodies

Cell fusions done three times produced hybridoma colonies in 2,500 wells. We cloned the hybridomas from wells with high  $\beta$ -Gal activity by limiting dilution, because the  $\beta$ -Gal activity of each well reflected the transfection efficiency into PC-3 cells via the antigen recognized by the antibodies secreted from the hybridoma. We thereby established hybridomas secreting mAb 1B7, 2H7, 6F8, and 9B10. Isotypes of mAb 1B7, 2H7, and 6F8 were determined to be IgG1 kappa and, for mAb 9B10, IgG2a kappa.

### Identification of mAbs 1B7, 2H7, 6F8, and 9B10 Antigens

Biotinylated proteins were detected at 40 kDa by immunoprecipitation using mAb 1B7 (Fig. 2A). Silver stain detected the same proteins. The epithelial cell adhesion molecule (Ep-CAM) was detected by mass spectrometry (Fig. 2B,C). cDNA of Ep-CAM was transfected into 293 T cells. Flow cytometry revealed that mAb 1B7 reacted with transfectants expressing Ep-CAM (Fig. 2D). We therefore concluded that the antigen recognized by mAb 1B7 was Ep-CAM.

In immunoprecipitation using mAb 2H7, an 80 kDa protein was detected (Fig. 3A). The protein was identified as poliovirus receptor (CD155) by mass spectrometry (Fig. 3B,C). cDNA of human CD155 was transfected into CHO cells and mAb 2H7 reacted with cells expressing CD155 (Fig. 3D).

In immunoprecipitation using mAb 6F8, 110, and 50 kDa biotinylated proteins were detected (Fig. 4A). The 110 kDa silver-stained protein, which was sharper than the 50 kDa band, was extracted and analyzed by mass spectrometry (Fig. 4B,C). The protein was identified as Na,K-ATPase (Fig. 4B,C). We obtained the cDNAs of human Na,K-ATPase  $\alpha$ 1, Na,K-ATPase  $\alpha$ 2, Na, K-ATPase  $\alpha$ 3, Na,K-ATPase  $\alpha$ 4 transcript variant 2, Na, K-ATPase  $\beta$ 1, Na,K-ATPase  $\beta$ 2, and Na,K-ATPase  $\beta$ 3 to determine the antigens. Each cDNA was transfected into CHO cells and it was found that mAb6F8 reacted

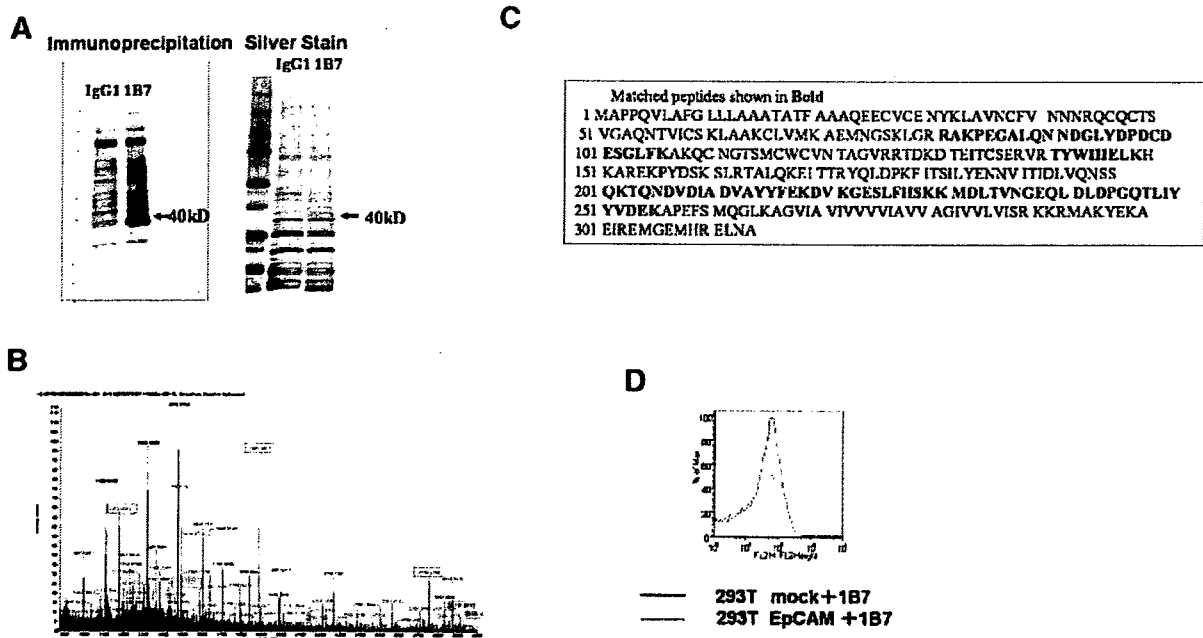


**Fig. 2.** Identification of mAb 1B7 antigen. **A:** Lysates of PC-3 cells were immunoprecipitated with mAb 1B7; proteins (40 kDa) were detected. The band that appeared at 40kDa (indicated by an arrow) was excised from the gel and analyzed by mass spectrometry. **B:** High-intensity spectra indicated by a rectangles indicate the peptide, the sequence of which corresponded to the amino acid sequence of human Ep-CAM. **C:** Boldface indicates the sequence of the detected peptide. **D:** Flow cytometry of the reactivity of mAb 1B7 with 293T cells transfected with cDNA of Ep-CAM. mAb 1B7 reacted only with 293T cells transfected with cDNA of Ep-CAM.

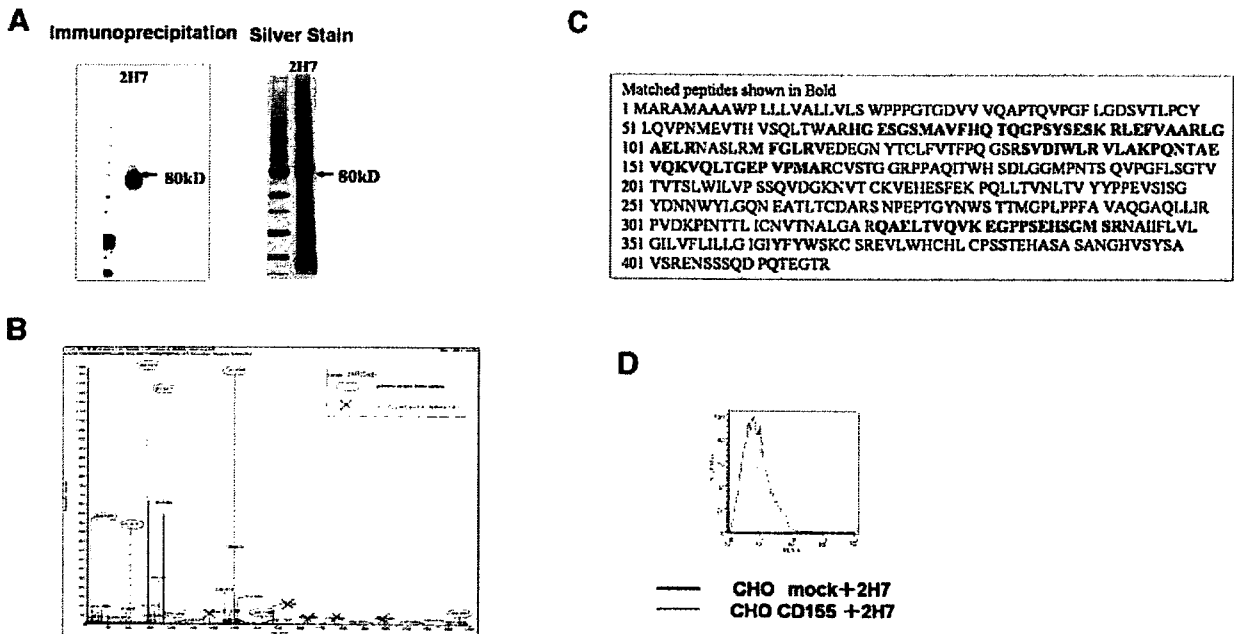


**Fig. 3.** Identification of mAb 2H7 antigen. **A:** Immunoprecipitation with mAb 2H7. The band that appeared at 80 kDa (indicated by an arrow) was excised from the gel and analyzed by mass spectrometry. **B:** Encircled high-intensity spectra indicate the peptide, the sequence of which corresponded to the amino acid sequence of human CD155. **C:** Boldface indicates the sequence of the detected peptide. **D:** Flow cytometry of the reactivity of mAb 2H7 with CHO cells transfected with cDNA of CD155. mAb 2H7 reacted only with CHO cells transfected with cDNA of CD155.

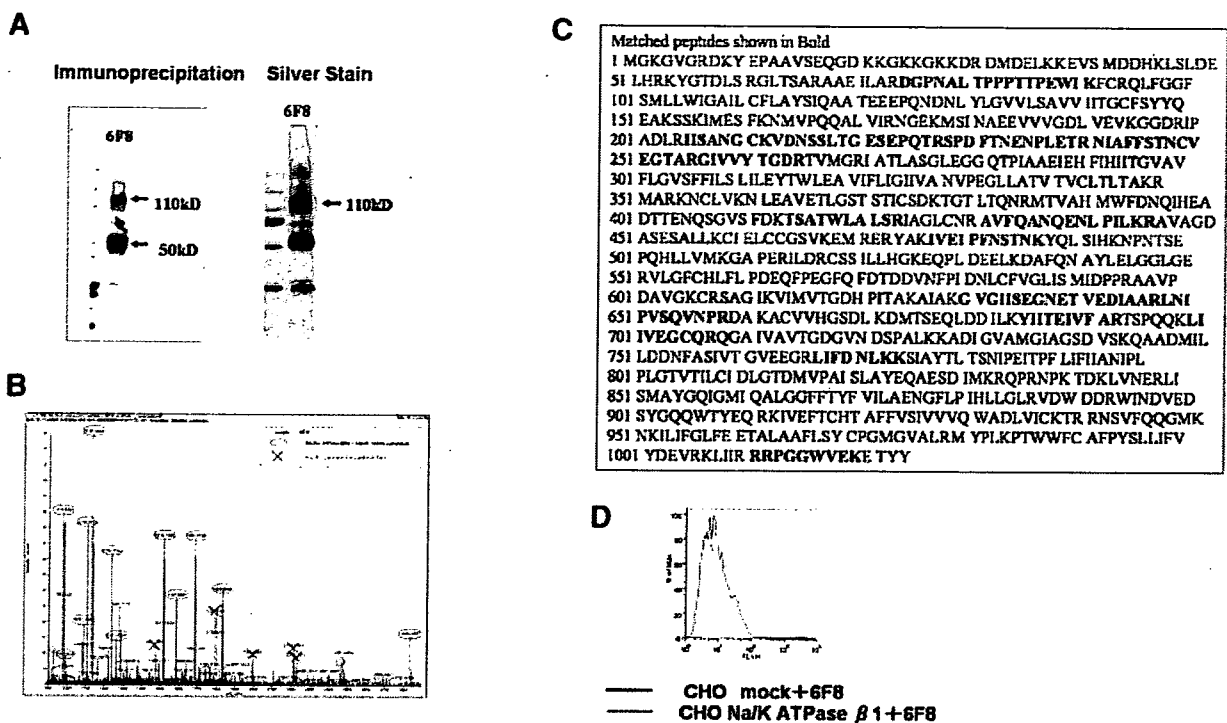


**Fig. 4.** Identification of mAb 6F8 antigen. **A:** immunoprecipitation with mAb 6F8; proteins (110 and 50 kDa) were detected. The band that appeared at 110 kDa was excised from the gel and analyzed by mass spectrometry. **B:** Encircled high-intensity spectra indicate the peptide, the sequence of which corresponded to the amino acid sequence of human Na,K-ATPase  $\alpha$ . **C:** Boldface indicates the sequence of the detected peptide. **D:** Flow cytometry of the reactivity of mAb 6F8 with CHO cells transfected with the cDNA of each subunit and isozyme of human Na,K-ATPase. mAb 6F8 reacted only with CHO cells transfected with cDNA of human Na,K-ATPase  $\beta$ 1.

only with the transfectant expressing the Na,K-ATPase  $\beta$ 1 subunit (Fig. 4D). We therefore concluded that the antigen recognized by mAb 6E3 was Na,K-ATPase  $\beta$ 1.

In immunoprecipitation using mAb 9B10, a 55 kDa protein was detected (Fig. 5A). The protein was identified as HAI-1 by mass spectrometry (Fig. 5B,C). cDNA of human hepatocyte growth factor activator inhibitor type 1 (HAI-1) transcript variant 2 and HAI-1 transcript variant 3 were obtained. Each cDNA was transfected into CHO cells. mAb 9B10 reacted with each transfectant (Fig. 5D). Therefore, we concluded that mAb 9B10 recognized HAI-1.

#### Transfection Efficiency Into PC-3 With mAbs and Adv-FZ33

**Flow cytometric analysis.** Transfection efficiency was evaluated with various mAbs. Cells transfected using AdvEGFP-FZ33 together with mAb 1B7, 2H7, 6F8, and 9B10 showed enhanced expression EGFP compared with those together with mouse IgG1 (Fig. 6A).

**Chemiluminescent  $\beta$ -Gal reporter gene assay.**  $\beta$ -Gal activity in mAb 1B7, 2H7, and 6F8 at the concentration

1.0  $\mu$ g/ml showed about 70-fold enhancement compared with control mouse IgG1. In mAb 9B10, transfection efficiency showed about 10-fold enhancement (Fig. 6B). Adv LacZ-FZ33 with mAb 6F8 showed significantly high expression of  $\beta$ -Gal compared with wild type—fiber adenovirus with or without mAb (Fig. 6C).

#### Distribution of Target Antigens

**Expression in several cell lines.** We examined the reactivities of mAb 1B7, 2H7, 6F8, and 9B10 with cancer and non-cancer cell lines by flow cytometry. mAb 2H7 and 6F8 reacted strongly with all cell lines (Fig. 7B,C). mAb 1B7 reacted with all cancer cell lines but not with PrMFB and PDF (Fig. 7A). mAb 9B10 did not react with SKOV-3, PrMFB, or PDF (Fig. 7D).

**Histologic findings on the specimens.** All of the prostate cancer cells (Fig. 8A,C) and most of the normal epithelial cells (Fig. 8B) showed strong immunoreactivity for mAb 1B7 in all the samples. Some of the normal epithelial cells (Fig. 8C,D) and all of the stromal cells (Fig. 8A–D) showed negative staining. No samples were stained with the other three mAbs.

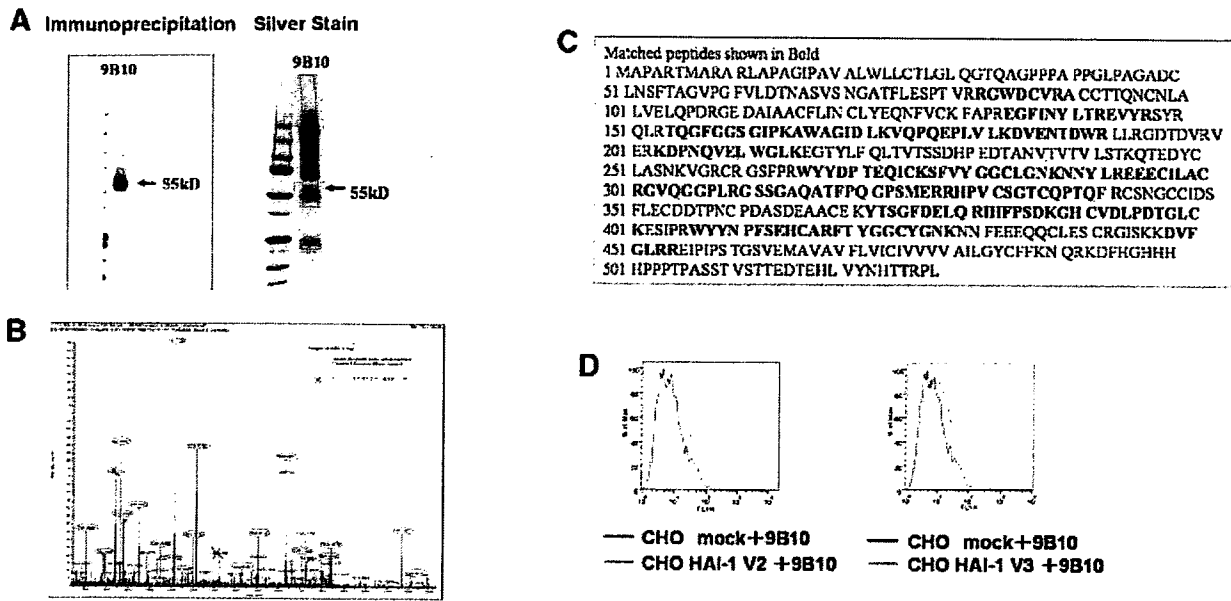


**Fig. 5.** Identification of mAb 9B10 antigen. **A:** immunoprecipitation with mAb 9B10. The band that appeared at 55 kDa (indicated by an arrow) was excised from the gel and analyzed by mass spectrometry. **B:** Encircled high-intensity spectra circle indicate the peptide, the sequence of which corresponded to the amino acid sequence of human HAI-1. **C:** Boldface indicates the sequence of the detected peptide. **D:** Flow cytometry of the reactivity of mAb 9B10 with CHO cells transfected with cDNA of each subunit of HAI-1. mAb 9B10 reacted with CHO cells transfected with cDNA of each subunit of HAI-1.

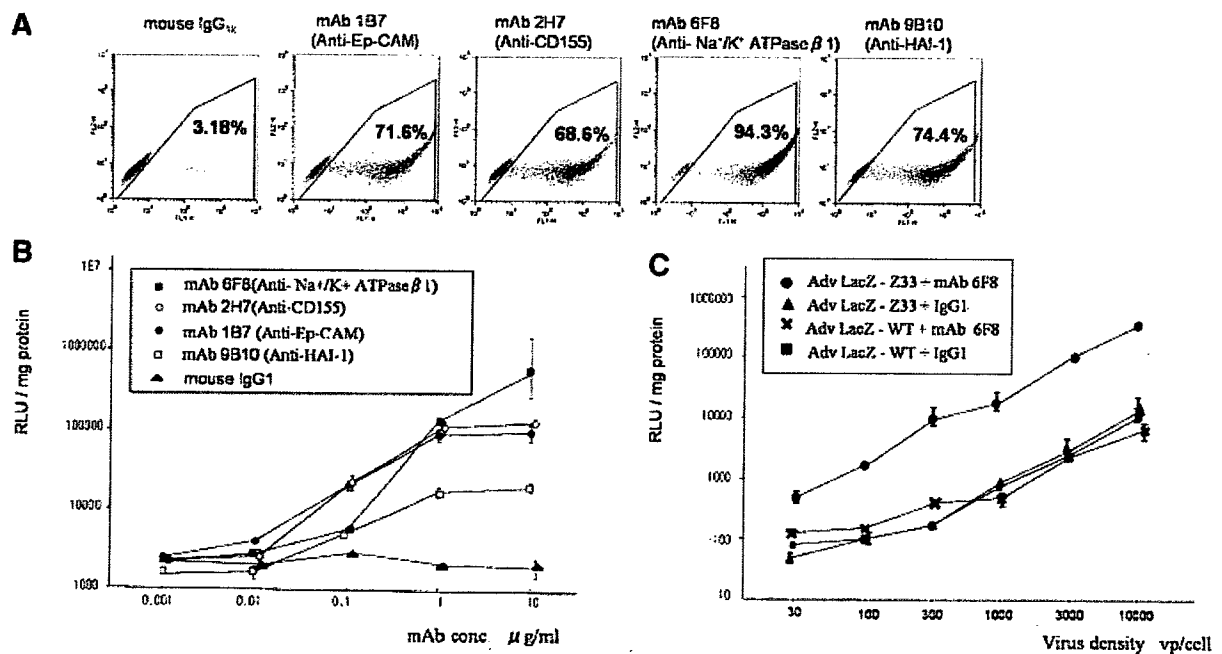


**Fig. 6.** Transfection efficiency into PC-3 cells with each fiber mutant adenovirus-mediated mAb. **A:** Numbers presented in each panel indicate the percentage of cells expressing EGFP. Cells transfected using AdvEGFP-FZ33 together with mIgG1 showed low expression of EGFP. Cells transfected using AdvEGFP-FZ33 together with mAbs 1B7(anti-Ep-CAM mAb), 2H7(anti-CD155 mAb), 6F8(Na,K-ATPase β 1 mAb), and 9B10(anti-HAI-1 mAb) showed enhanced expression of EGFP. **B:** The cells were lysed, and assayed for β-Gal activity using a commercial kit (n = 4). AdvEGFP-FZ33 together with mAbs 1B7, 2H7, 6F8, and 9B10 showed high transduction efficiency compare with control IgG. **C:** Adv LacZ - FZ33 together with mAb 6F8 showed high transduction efficiency compared with wild type adenovirus (Adv LacZ-WT).